First Forbidden Nonunique Beta Transitions in Re^{186}†

F. T. PORTER, M. S. FREEDMAN, T. B. NOVEY, AND F. WAGNER, JR.
Argonne National Laboratory, Lemont, Illinois

(Received January 9, 1956)

The beta spectrum of the main inner group of 89.0-hr Re^{186} ($E_0=934.3\pm1.3$ kev; 24% of total betas; $\log ft=8.0$) has been magnetically analyzed in coincidence with the 137.2-kev gamma. The observed spectrum does not have the allowed shape nor the unique ($\Delta I=2$, yes) shape; its spectrum shape correction factor increases about 18% from 150 kev to 900 kev. Subtraction of this spectrum, weighted with its measured relative abundance, from the composite spectrum, produces the spectrum of the ground state transition ($E_0=1071.5\pm1.3$ kev; 76% of total betas; $\log ft=7.68$). Its similarly nonallowed, nonunique shape factor increases by about 22% from 150 kev to 1050 kev. Both transitions are interpreted as first forbidden ($\Delta I=1$, yes); Re^{186} is assigned a ground state spin and parity $1(-)$. A theoretical parametric fitting of these spectra with the combination of scalar and tensor beta interactions is demonstrated; the limited ranges of the fitting parameters, which are functions of the nuclear matrix elements, are obtained.

A comparison is presented between the theoretical fittings of the beta spectrum of the inner group and of the beta-gamma angular correlation.

Pursuant to these studies on Re^{186} we obtained values for the maximum beta energies, gamma energies, conversion coefficients, half-life, and branching ratios, particularly of the approximately 0.1% abundant 307-kev beta group.

I. INTRODUCTION AND SUMMARY

MOST of the first forbidden β transitions involving nuclear spin changes of zero or one have experimentally the allowed ("statistical") shape.[1] The notable exception, Bi^{210} (RaE) has recently been discussed extensively[2–4]; only with the presumption that $\Delta I=1$ rather than 0 has the experimental spectral shape been fitted in a satisfactory way (with a combination of scalar and tensor interaction). The other exception is the 2.317-Mev β transition in Sb^{124},[5] which also exhibits a β-γ directional anisotropy.[6–8] The nuclear parameters which account for the shape of the β spectrum are not inconsistent[9] with those fitting the β-γ correlation for the combination ST and $\Delta I=1$, in the theoretical approximation $\alpha Z\ll1$.

It has been pointed out[1,2] that only in the case of accidental cancellation of the usually dominant energy independent terms (Coulomb terms $\propto\alpha Z/2R$) in the spectrum shape correction factor will the energy dependence of the smaller terms be exhibited. If one fairly expects that present day β spectroscopy is capable of detecting 3 to 5% deviations from the statistical shape, then theory[10] leads one to expect that deviations from statistical shapes should not be as infrequent as seems to be true thus far.

Moreover, as has been pointed out,[11] in decays in which β-γ directional anisotropy exists, the associated β spectrum must deviate from the statistical shape, although Fuchs[12] has shown that this deviation may be small. Of the several known cases of β-γ anisotropy,[13–18] K^{42}, As^{76}, Rb^{86}, Sb^{122}, Sb^{124}, I^{126}, Tm^{170}, the associated spectra of all but Sb^{124} have been reported to have the statistical distribution. All the others except Tm^{170} are believed to beta decay from a $2(-)$ parent state to a $2(+)$ excited state of the even-even daughter and thus are $\Delta I=0$ first-forbidden transitions followed by $E2$ transitions. Tm^{170} differs only in having a $1(-)$ ground state.[18] Hence $\Delta I=1$ for the inner group beta transition, which has an allowed shape associated with a β-γ

† Based on work performed under the auspices of the U. S. Atomic Energy Commission.

[1] H. M. Mahmoud and E. J. Konopinski, Phys. Rev. **88**, 1266 (1952).
[2] M. Yamada, Progr. Theoret. Phys. (Japan) **10**, 252 (1953).
[3] E. A. Plassmann and L. M. Langer, Phys. Rev. **96**, 1593 (1954).
[4] G. E. Lee-Whiting, Phys. Rev. **97**, 463 (1955).
[5] Langer, Lazar, and Moffet, Phys. Rev. **91**, 338 (1953); J. Moreau, Compt. rend. **239**, 800 (1954). This transition is uncomplicated by lower energy betas only above 1.60 Mev.
[6] E. K. Darby and W. Opechowski, Phys. Rev. **83**, 676 (1951).
[7] D. T. Stevenson and M. Deutsch, Phys. Rev. **83**, 1202 (1951).
[8] Kloepper, Lennox, and Wiedenbeck, Phys. Rev. **88**, 695 (1952).
[9] M. Morita and M. Yamada, Progr. Theoret. Phys. (Japan) **8**, 449 (1952); **10**, 641 (1953).
[10] Using Eq. (8) of reference 1 with $W_0=2$ and $\alpha Z/2R\approx10$, one expects deviations of the order of 3% for (estimated) $x\approx y\approx1$, $\Delta I=1$.
[11] D. L. Falkoff and G. E. Uhlenbeck, Phys. Rev. **79**, 334 (1950); L. C. Biedenharn and M. E. Rose, Revs. Modern Phys. **25**, 729 (1953); H. Frauenfelder, in *Beta- and Gamma-Ray Spectroscopy*, edited by Kai Siegbahn (Interscience Publishers, Inc., New York, 1955), p. 570.
[12] M. Fuchs, Ph.D. dissertation, University of Michigan, 1951 (unpublished).
[13] K^{42}; $\beta\gamma(\theta)$—D. T. Stevenson and M. Deutsch, Phys. Rev. **84**, 1071 (1951); shape—Koerts, Schwarzschild, Gold, and Wu, Phys. Rev. **95**, 612(A) (1954).
[14] As^{76}; $\beta\gamma(\theta)$—H. Rose, Phil. Mag. **44**, 739 (1953); S. L. Ridgeway and F. M. Pipkin, Phys. Rev. **87**, 202 (1952); shape—E. P. Tomlinson and S. L. Ridgeway, Phys. Rev. **88**, 170 (1952); E. N. Jensen, Ames Laboratory Report, ISC-533, 1954 (unpublished).
[15] Rb^{86}; $\beta\gamma(\theta)$—D. T. Stevenson and M. Deutsch, Phys. Rev. **83**, 1202 (1951); shape—Pohm, Lewis, Talboy, and Jensen, Phys. Rev. **95**, 1523 (1954).
[16] Sb^{122}; $\beta\gamma(\theta)$—I. Shaknov, Phys. Rev. **83**, 333(A) (1951); shape—M. J. Glaubman, Phys. Rev. **98**, 645 (1955).
[17] I^{126}; $\beta\gamma(\theta)$—D. T. Stevenson and M. Deutsch, Phys. Rev. **84**, 1021 (1951); shape—Mitchell, Mei, Maienschein, and Peacock, Phys. Rev. **76**, 1450 (1949); Koerts, Macklin, Farrelly, Van Lieshout, and Wu, Phys. Rev. **98**, 1230 (1955).
[18] Tm^{170}; $\beta\gamma(\theta)$—T. B. Novey, Phys. Rev. **78**, 66 (1950); H. Rose, Phil. Mag. **43**, 1146 (1952); shape—Graham, Wolfson, and Bell, Can. J. Phys. **30**, 459 (1952); Pohm, Lewis, Talboy, and Jensen, reference 15; R. Richmond and H. Rose, Phil. Mag. **43**, 367 (1952).

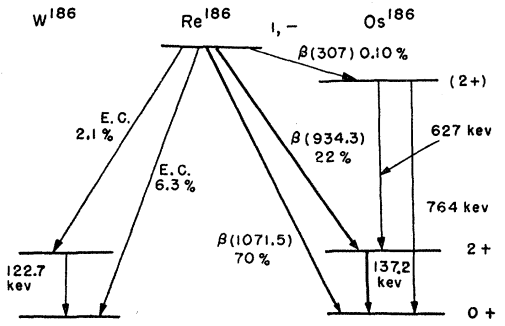

FIG. 1. Decay scheme of Re^{186} including results of the present work.

anisotropy. Fujita, Morita, and Yamada[19] have shown that for Tm^{170}, the nuclear parameters which produce a fit for the differential β-γ anisotropy permit, but do not require, a spectral shape which deviates by only a few percent from the allowed distribution. We judge that this slight "shape" might be within the uncertainties of the experiments. Sb^{124} is the only other case also believed to be $\Delta I=1$; it, as noted above, has a nonallowed shape.

In the present paper we consider the related case of Re^{186}. Previous investigators[20] had established the basic features of the decay scheme as given in Fig. 1 with general agreement that both abundant beta branches have allowed shape. This led to the assignment of $1(-)$ for the ground state of Re^{186}. King[21] has pointed out that this assignment would violate Nordheim's rule which would predict spin 2 and hence a unique shape for the ground state transition.

The first indication that at least one of the β spectral shapes is not allowed came from Guss, Killion, and Porter[22] who reported that if the ground state β transition was assumed to have the allowed shape, then the 934-kev group obtained by subtraction exhibited a shape which could be fitted with the unique first forbidden correction factor ($\Delta I=2$, yes), supporting a $0(-)$ assignment. At the same time, Hurley and Jastram[23] reported that the β-γ directional correlation was isotropic ($A<0.07$). These results are incompatable in the light of β-γ correlation theory which predicts an integral anisotropy of about 0.4 for the β-γ cascade $(0-, 2+, 0+)$. It appeared that a resolution of the problem hinged on a determination of the shape of the first inner group which would be independent of assumptions as to the nature of the ground-state transition, i.e., by coincidence spectroscopy.

In the interests of continuity we summarize the results of these experiments briefly here.[24] We have observed nonunique, nonallowed, and very similar shapes for both the first inner group and the ground state beta transitions in Re^{186}. These are interpreted as first forbidden transitions with $\Delta I=1$, requiring a spin assignment, as originally proposed by Metzger and Hill[20] and by Steffen[20] of $1(-)$ for the Re^{186} ground state. The integral and differential β-γ directional anisotropy has been measured.[25] The integral ($E_\beta=257$–934 kev) anisotropy of $0.105(\pm 0.003)$ and the maximum differential anisotropy of 0.158 (for $E_\beta=934$ kev) are both too small to be associated with a $\Delta I=2$, yes beta transition. Both the beta spectra and the differential directional correlation can be reconciled with theory, in an internally consistent fashion for the theoretical approximation used.

II. APPARATUS

Spectrometer

The beta spectroscopy described here involves both coincidence operation and the usual (singles) manner of operation. The Argonne double lens spectrometer[26,27] was operated in two different modes in the present experiments. One mode, used in coincidence studies, is characterized by a measured transmission of 5% (of 4π steradians) and a momentum resolution of 6.7% (width at half-height) for a source diameter of 6 mm; the other mode has a transmission of 0.8% and a resolution of 2.0% with a source diameter of 3 mm.

β Detectors

One of the two types of beta particle detectors used was an end-window, loop-type, continuous-flow proportional counter using research grade propane at 18 cm Hg pressure. The window for these experiments, 0.92 mg/cm² Mylar, with measured cutoff of 19 kev, was unsupported over the 1-cm diameter aperture. In these experiments we are interested in beta energies greater than 150 kev. Plateaus 200 volts long were realized with slope of 1% per 100 volts for high-energy (low pulse amplitude) beta particles.

The other beta particle detector was a scintillation counter. Although both detectors were used in the coincidence experiments, emphasis is placed on the results obtained with the scintillation detector. The light output of the 1 mm thick×11 mm diameter anthracene disk (covered by 200 μg/cm² aluminum foil reflector),

[19] Fujita, Morita, and Yamada, Progr. Theoret. Phys. (Japan) **11**, 219 (1954).
[20] F. R. Metzger and R. D. Hill, Phys. Rev. **82**, 646 (1951); R. M. Steffen, Phys. Rev. **82**, 827 (1951).
[21] R. W. King, dissertation, Washington University, 1952 (unpublished).
[22] Guss, Killion, and Porter, Phys. Rev. **95**, 627(A) (1954).
[23] J. P. Hurley and P. S. Jastram, Phys. Rev. **95**, 627(A) (1954).
[24] Preliminary reports of this work have appeared: Porter, Freedman, Novey, and Wagner, Phys. Rev. **98**, 214 (1955); **99**, 671(A) (1955).
[25] Novey, Freedman, Porter, and Wagner, Phys. Rev. **103**, 942 (1956) following paper.
[26] Space limitations prevent an extended discussion of many of the details of this paper. Reference should be made to Argonne National Laboratory Report 5525, 1956 (unpublished). Copies of this report may be purchased from the Office of Technical Services, Department of Commerce, Washington 25, D. C.
[27] The coils and current control are discussed by Freedman, Ramler, and Smaller, Rev. Sci. Instr. **23**, 571 (1952); and by J. Wolff and M. S. Freedman, Rev. Sci. Instr. **22**, 736 (1951).

was led out of the strong magnetic field region by a Lucite light pipe 24 in. long by 1 in. o.d. to a Dumont 6292 photomultiplier tube, cooled to −80°C. Double shell magnetic shielding (Mu metal) around the phototube was sufficient to insure that the phototube performance was not affected (<1% variation) by the magnetic field of the spectrometer.

The question of the relative efficiency of the scintillation detector for beta particles over the energy range of interest (>150 kev), has been approached in three ways. The first involved pulse-height analysis of the output of the scintillation detector; the second was a direct comparison of the anthracene counter to the proportional counter; the third was the performance in the spectrometer with spectra of known shape. We present the first of these in some detail because the knowledge of the pulse-height distribution from the scintillation beta detector is necessary for some of the later comments on the over-all coincidence efficiency.

Figures 2 and 3 show the pulse amplitude distribution from the anthracene beta detector as electrons of various indicated energies are focused from a beta continuum onto the crystal by the spectrometer. We include one example at 104 kev which is below the limit of our interest, 150 kev. Note that at energies over 370 kev the pulse-height distribution is "double peaked." The peaks near 300 bias units are interpreted as those from electrons which penetrate the 1-mm crystal without large-angle scattering except that the 370-kev electrons do not quite penetrate the crystal. The higher broad "peak" is due to electrons with path lengths in the crystal which, because of scattering, exceed the minimum length, about 1 mm, by various amounts. The rise at low bias, which has been shown to originate in anomalous afterpulses in the phototube extending far beyond the analyzer dead time of 8 microseconds, is shown only for the 150-kev electrons, but it exists for all incident energies. The backscattering "tail" and afterpulse rise of the beta pulse-height distribution are obscured by the large room temperature background of the phototube, but at −80°C they are distinct. The integral background of 12 000 counts/min above the discrimination level, 10 bias units, is reduced to 500/min with cooling. In the interest of maximum gain, we operated with the highest phototube voltage (1015 volts) consistent with a clean separation from afterpulses[26] at low pulse amplitude. At this voltage the sharp rise in afterpulse distribution occurs below 8 bias units for all energies and so we reject them by discriminating at 10 bias units. In so doing, we must inevitably lose some small fraction of the real pulses, the fraction thus lost depending on the beta energy. We compute the singles efficiency η by extrapolating the flat low tail on the pulse-height distributions to zero amplitude. Above 150 kev the relative efficiency is greater than 99% and is known with an accuracy of 0.1%. This operating point of 10 bias units corresponds, as expected, to the upper end of gain and bias plateaus (flat to within <1% for fivefold bias increases).

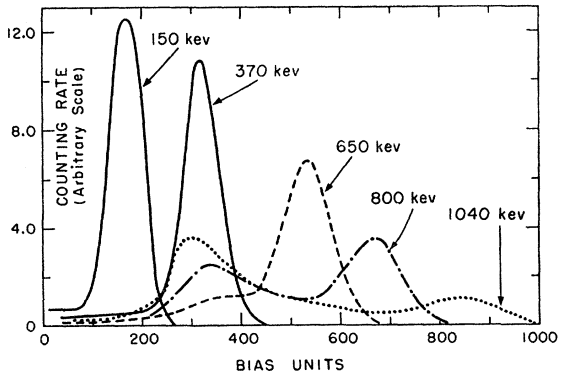

FIG. 2. Pulse-height distributions for beta particles of indicated energy focused on 1-mm-thick anthracene disk in spectrometer. Figure 3 shows expansion of low pulse height region. All curves are normalized to the same area.

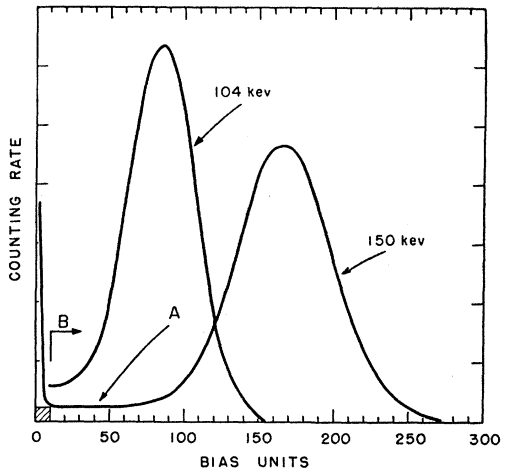

FIG. 3. Pulse-height distributions for beta particles of indicated energy focused on 1-mm-thick anthracene disk in spectrometer. Photomultiplier at −80°C. Upturn below 8 bias units due mainly to afterpulses; the background (source out) has been subtracted. Flat tail *A* due to beta particles backscattered from crystal. *B* indicates beta pulse-analyzer discrimination level (10 bias units). Shaded rectangle designates assumed loss of single counts for 150-kev beta particles due to discrimination at *B*.

For the second check on the scintillation counter efficiency, the counting rate of the anthracene detector was compared directly with that of the proportional counter at various energies from 100 kev to 700 kev by interchanging the two via the detector vacuum lock with the same sample in the spectrometer. A detector baffle limited the image diameter to 7 mm, less than the the respective detector apertures. This experiment showed that within the experimental error of the comparison (0.8%), the relative efficiency of the scintillation counter was the same as the calculated from the pulse-height distributions.

Finally, independent evidence that the scintillation

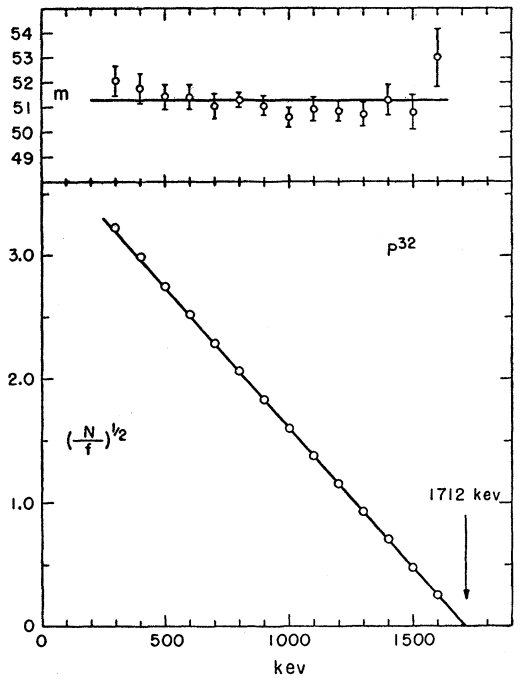

FIG. 4. Kurie and m plots for P^{32} with proportional-counter detector; spectrometer transmission = 5%. The straight line in the m plot is drawn at the average ordinate of the points.

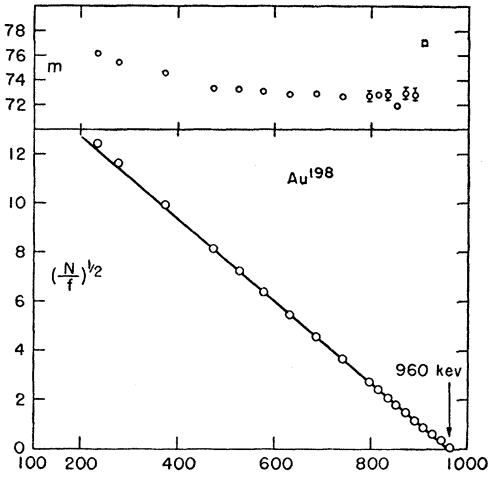

FIG. 5. Kurie and m plots for Au^{198} with proportional-counter detector; spectrometer transmission = 5%. Statistical error smaller than circle unless indicated.

detector efficiency is known accurately is the performance with known spectra. This performance is not independent of other characteristics of the magnetic spectrometer. However, the fact that straight Kurie plots were obtained for both P^{32}, 300–1712 kev (Fig. 4) and Au^{198}, 400–960 kev (Fig. 5) employing the proportional counter detector and also for Au^{198} (Fig. 11) using the scintillation counter supports both the performance of the magnetic lens spectrometer as an instrument for determining spectral distributions and the essentially constant efficiency of the scintillation counter over this energy range. A discussion of the slight upturn in the Au^{198} Kurie plots is given in Sec. IV.

Gamma Detector and Source Mounts

The gamma detector is a NaI(Tl) crystal, $\frac{3}{4}$ inch in diameter and $\frac{3}{4}$-inch long, located one inch behind the source on the axis of the spectrometer. Light pipe and magnetic shielding are the same as for the beta detector.

The absence of significant scattering from the whole coincidence source holder is illustrated by the spectrum of P^{32} which is presumed to have the statistical shape.[28] Figure 4 gives the Kurie plot and m function[29] of P^{32} taken with the coincidence source holder and proportional counter beta detector. The source was vacuum volatilized H_3PO_4($\sim$40 μg/cm^2) on 200 μg/cm^2 Al, $\frac{1}{4}$-inch diameter; the spectrometer was set to 5% transmission. The resolution correction[26] was made by applying constants derived from the line shape of the Re^{186} 63-kev K-conversion line (from another experiment). We do not present data below 300 kev because of the presence of P^{33} in the sample. Inspection of the figure, particularily the m function, indicates a maximum possible scattering component of 2% at about 300 kev, $<E_0/5$.

Coincidence Circuit

Figure 6 shows a block diagram of the fast-slow coincidence arrangment used for the coincidence beta spectrum.[30] Saturated pulses are shaped with 30-mμsec (double travel times) delay lines and are fed to the fast-coincidence circuit of the Garwin type.[31] With this shaping and the extremely high gain used to oversaturate the pulses, the measured resolution time, $2\tau_f$, is the order of 0.12 μsec.[26]

Pulse amplitude selection is accomplished by demanding triple coincidences between the output of the fast-coincidence circuit and the outputs of the relatively slow, well stabilized pulse-height analyzers[32] (operated either differentially or integrally) in the beta and gamma channels. We record triple coincidences (T), double coincidences (D), analyzed betas (B), analyzed gammas (G), unanalyzed betas (β), and unanalyzed gammas (γ).

[28] Sheline, Holtzman, and Fan, Phys. Rev. **83**, 919 (1951).

[29] In the notation of J. P. Davidson and D. C. Peaslee, Phys. Rev. **91**, 1232 (1953), $m=N/[f(E_0-E)^2]$, the experimental spectrum shape factor; f, the Fermi Coulomb function as given in the Bureau of Standards tables, includes the usual factor p^2. With an accurately known end-point value, E_0, the m function provides a much more sensitive way of displaying small deviations from the allowed shape than does the conventional Kurie plot.

[30] When the proportional counter was the beta detector, the so-called "jitter time" necessitated the use of shaping times for the β and γ pulses about twice as long as for the scintillation detector in order to insure 100% coincidence efficiency.

[31] R. L. Garwin, Rev. Sci. Instr. **24**, 618 (1953).

[32] R. K. Swank, Argonne National Laboratory Report ANL-4303, 1949 (unpublished), describes both the linear amplifier and the pulse-height analyzer.

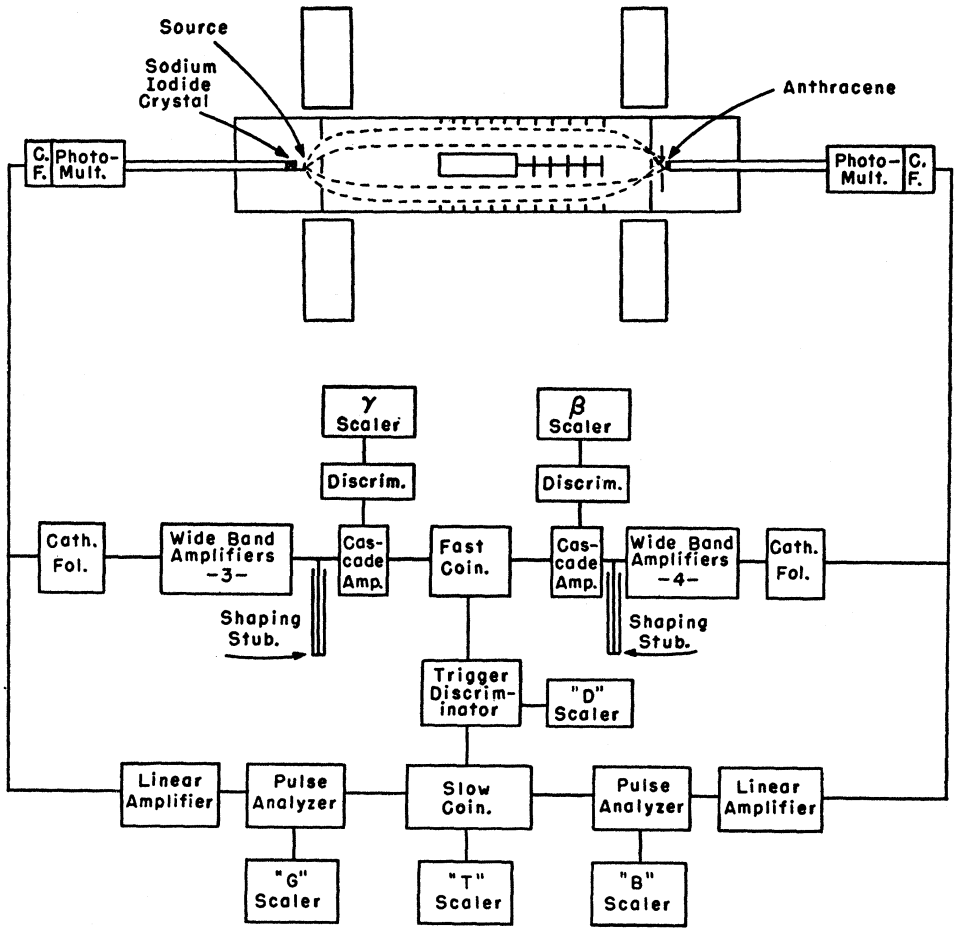

FIG. 6. Block diagram of coincidence circuit and spectrometer.

Coincidence Efficiency

A question of prime importance for beta coincidence spectroscopy is that of the relative coincidence efficiency as a function of beta energy. The crux of the problem is that the detectors, particularly the beta detector, put out a broad distribution of pulse amplitudes rather than a single pulse amplitude, and that, moreover (Figs. 2 and 3), this distribution changes with beta energy and extends to a small extent down into the noise background and afterpulse region. A criterion for 100% coincidence efficiency that is often used is the existence of a flat-top delay curve.[33] With coincidence rates of the order of a few hundred per minute, it is not practical to determine the "flatness" of the delay curves to the required accuracy.[26]

Another approach we have used is to demand that the real coincidence rate be independent of the fast-amplifier gains above a certain minimum. Gains above these minima insure that the fast-coincidence circuit will respond to every pulse which is recorded by B and G. Practically, one cannot realize flat gain plateaus if one must detect even moderately low-energy pulses[26] and one must substitute for the goal of 100% coincidence efficiency the attainment of a high, measurable, and hence correctable, efficiency.

Although the requirements of flat-top delay curves and gain plateaus were useful in the early exploration of the apparatus and in establishing optimal values for the delays and gains to be used, the quantitative answer to the question of relative coincidence efficiency was obtained by examining the number of real coincidences per B as a function of pulse height (not energy) selected differentially with the pulse-height analyzer. These experiments showed that the number of real coincidences per B was independent of beta pulse height for pulse heights above 60 bias divisions (refer to Figs. 2 and 3 for bias unit scale). Figure 7 shows this differential efficiency curve in the region below 60 bias divisions. In this figure we call 100% coincidence efficiency the constant value of reals/B[34] obtained for

[33] Bell, Graham, and Petch, Can. J. Phys. **30**, 35 (1952).

[34] The B scaler was driven by the same trigger-generated pulse that was impressed on the triple mixer grid, and similarly for G. Thus any count recorded as B has been effective in questioning the triple coincidence circuit. By "reals" we mean real triple coincidences.

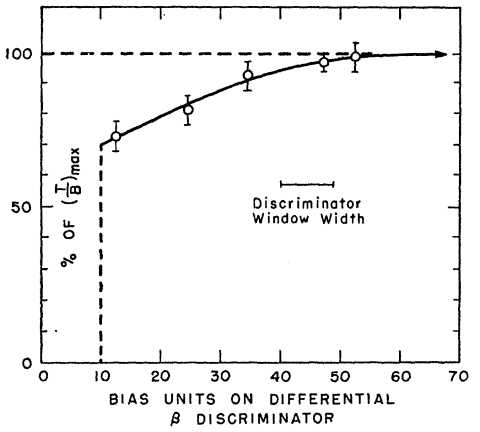

FIG. 7. Differential coincidence efficiency applicable for any beta energy, focused by the spectrometer. This curve is used in determining the over-all coincidence efficiency. The ordinate is the ratio of the triple coincidences (T) to the beta particles recorded (B) with those pulse heights indicated on the abscissa, expressed as percent of the maximum observed. Above 60 bias units, the ratio T/B was observed to be independent of the beta pulse height. Bias units are the same as in Figs. 2 and 3. The differential coincidence efficiency value used in computing the over-all coincidence efficiency is taken to be zero below 10 bias units, since the B discriminator is adjusted to count integrally above 10 bias units during an actual spectrum run.

pulse heights over 60 bias units. Since the B pulse-height discriminator was operated as an integral discriminator during a spectrum run, accepting only pulse heights over 10 bias units, the efficiency must be taken as zero below 10 bias units. This differential efficiency curve convoluted with the pulse-height distribution of Figs. 2 and 3 (with tails extrapolated as above) was used to obtain the over-all coincidence efficiency as a function of beta energy (Fig. 8). Note that because the sytems has an efficiency so near 100%, the over-all coincidence efficiency can be given to 0.1%, even with the uncertainties of the order of 5% in the low-energy part of the differential efficiency curve.

The resolving time ($2\tau_f$) of the coincidence circuit can be determined in three ways: (1) chance rate measurement with independent sources; (2) chance rate measurement with single source in which the real coincidences are eliminated by use of a sufficiently long relative delay; and (3) measurement of the effective width[35] of the delay curve for real coincidences. Of these, we have used the more fundamental independent-source technique to investigate the dependence of $2\tau_f$ on the beta energy. Figure 9 shows the result of these measurements for the anthracene detector. Because of its convenience, we used the delay method during the run to monitor the stability of $2\tau_f$. We have not been able to demonstrate conclusively any difference in $2\tau_f$ as measured by the two methods in our apparatus. During the spectrum runs, we monitored $2\tau_f$ at one energy which is near the peak of the beta spectrum and which is on the flat part of the curve of $2\tau_f$ *vs* beta energy. The curve of $2\tau_f$ *vs* beta energy was then normalized to the value obtained during the actual run. We have not found any evidence for drift in $2\tau_f$ during three day runs, but changes of the order of 5% have been noted over periods of several weeks. In summary, our knowledge of $2\tau_f$ at a particular time for a particular beta energy has at most a 5% uncertainty. Since we used source strengths small enough so that the ratio reals/chance was greater than 10 over most of the spectrum, the error due to the uncertainty in $2\tau_f$ was reduced to less than 0.5%.

[35] Bell, Graham, and Petch, reference 33, define effective width as the area of the delay curve divided by the height. The resolving time so defined will be inconsistent with the results of measurement with independent sources unless the coincidence efficiency is 100% at the peak of the delay curve; see Bay, Henri, and Kanner, Phys. Rev. **100**, 1197 (1955).

III. TREATMENT OF DATA

Calculation of Real Coincidences

The treatment of the raw coincidence data to produce a value for the real coincidence rate, R, and for the coincidence momentum spectrum, $M(p)$, is given in Eqs. (1); these represent a degree of approximation which is more than sufficient for most present day coincidence beta spectroscopy. The special effects given consideration are the coincidence efficiency, ϵ, a chance rate, C_s, peculiar to a fast-slow coincidence combination such as ours, and also some usually disregarded dead-time effects. Many of these effects are very small for our circuits, but might not be for others. However, in view of the small effects sought in the present experiments, we have included these small corrections.[26,36]

$$R=T_c-2\tau_f^*(B^*-R')(G^*-R'), \tag{1a}$$

$$T_c=(T/\epsilon-C_s)(1+\delta_B{}^cB)(1+\delta_G{}^cG), \tag{1b}$$

$$C_s=(D-T)G2\tau_s, \tag{1c}$$

$$R'=T/\epsilon-2\tau_fGB, \tag{1d}$$

$$B^*=B(1+\delta_BB), \tag{1e}$$

$$G^*=G(1+\delta_GG), \tag{1f}$$

$$2\tau_f^*=2\tau_f\frac{(1+\delta_B{}^cB_\tau)(1+\delta_G{}^cG_\tau)}{(1+\delta_BB_\tau)(1+\delta_GG_\tau)};\quad 2\tau_f=\frac{T}{B_\tau G_\tau}, \tag{1g}$$

$$M(p)=\frac{R}{(G-bg)p}. \tag{1h}$$

The quantities are defined as follows: R=real coincidence rate; R'=first approximation of R; B and G =observed analyzed beta rate and analyzed gamma rate; bg=appropriate background; T=observed triple

[36] See Westcott, Greenberg, and Kirkaldy, Can. J. Phys. **31**, 859 (1953) for a discussion of some of these and higher order corrections.

coincidence rate; T_c=triples rate corrected for coincidence efficiency, slow chance events, and dead time losses; D=observed double coincidence rate; ϵ=intrinsic coincidence efficiency, ≤ 1, in general a function of beta energy (see Fig. 8); $2\tau_{fs}$=resolving time of the slow (triple) coincidence circuit for G pulses and D-B pairs (2.5 μsec); $2\tau_f$=observed resolving time of fast (double) coincidence circuit measured with rates B_τ and G_τ [in general, a function of beta energy (see Fig. 9)]; δ_B and δ_G=effective dead time of B channel and of the G channel (8.0 and 5.9 μsec); $\delta_B{}^C$ and $\delta_G{}^C$ =effective dead time for triple coincidences of the B and G channels (6.3 and 3.6 μsec); $M(p)$=observed coincidence momentum distribution; p=electron momentum.

The asterisk denotes dead-time-corrected quantities. Dead-time corrections [e.g., Eqs. (1e) and (1f)] in our case are given well by the linear approximation.[37] The dead-time-correction factors of the form $(1+\delta_B B)$ are usually between 1 and 1.01. The measurement of the fast resolving time $2\tau_f$ has been discussed previously.

The real coincidence rate R is obtained in Eq. (1a) in which the second term represents the fast chance coincidences, and T_c is the triple coincidence rate corrected [Eq. (1b)] for coincidence efficiency (ϵ), resolving time losses, and slow chance rate C_s [Eq. (1c)]. C_s is always less than 0.2% T for our experiments. Equation (1d) for R' represents the usual approximation in treating coincidence data with the exception of the factor ϵ, the over-all coincidence efficiency. The ratio R/R' in these experiments lies in the range 0.99–1.02, for B and G rates of $<100\,000$ counts/min, and for the resolving times and dead times of this equipment.[26]

The coincidence rate R is divided by $(G-bg)$ to correct for small drifts in G-discriminator level. This eliminates the explicit correction for radioactive decay. Since the G-discriminator level is chosen in the trough between the photopeak and the Compton and/or x-ray distribution, small drifts in the G-discriminator level are expected to affect the G count only slightly. It is indeed observed that $(G-bg)$ follows the decay curve characteristic of the sample with fluctuations of $\pm 2\%$.

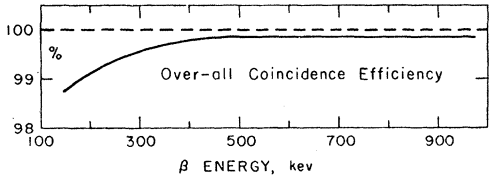

FIG. 8. Over-all coincidence efficiency as a function of beta-particle energy obtaining during the Re^{186} experiments. This curve is calculated from the observed differential efficiency curve of Fig. 7 in conjunction with the observed pulse-height distributions of Figs. 2 and 3.

[37] See for example L. G. Rainwater and C. S. Wu, Nucleonics 1, 60 (1947).

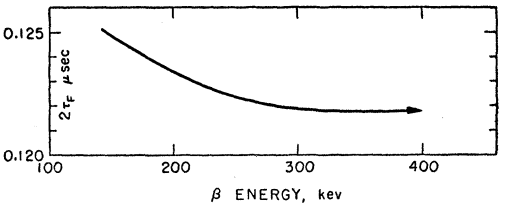

FIG. 9. Fast resolving time ($2\tau_f$) as a function of beta energy. Note the small increase in $2\tau_f$ at low beta energies. This behavior is observed with the anthracene scintillation counter as beta detector. No variation in $2\tau_f$ with beta energy is observed above beta energies of 300 kev.

Correction for Finite Resolution

$M(p)$ must be corrected for the finite momentum resolution of the spectrometer.[26,38] This correction expresses the true momentum distribution $N(p)$ in a series expansion in derivatives of the measured spectrum $M(p)$; the coefficients are derived by numerical integration from the empirical line shape ("transmission curve") of the spectrometer rather than from analytic approximations thereto. The analysis requires only that the line shape parameters be independent of the momentum as would be the case for a magnetic spectrometer with no scattering and for a thin source. This has been investigated experimentally by comparing in detail conversion line shapes at various energies, with sources of the same diameter, in the high transmission mode of operation of the spectrometer. The sources were all very thin with reference to the energies of the conversion lines of interest. The comparison showed that the K-conversion line at 63 kev in the decay of Re^{186} has very nearly the same shape as the 328-kev conversion line in the decay of Au^{198}, and as the 624-kev line in the decay of Cs^{137} (Fig. 10). In the first two examples, however, some uncertainties in the low-intensity wings of the lines is introduced by the necessity of subtracting the underlying beta continua. This comparison of the line shape parameters as a function of energy, which is the *only* point of concern for the spectrum resolution correction, cannot be made unequivocally using different sources,[26] because of small source distribution effects. However, since the differences in the line shapes are quite small, (those shown in Fig. 10, plus a number of others run with different Re^{186} and Au^{198} sources) and exhibit no trends with energy (down to 63 kev) such as might be expected, e.g., scattering tails at low energy, we assume that the parameters are independent of energy for such sources. We therefore apply the parameters as constants, but use those derived from a conversion line (if one exists) in the actual source to correct the spectrum of that source. The straightness of the Kurie plots of P^{32} and Au^{198} observed in the 5% transmission mode (Figs. 4,

[38] G. E. Owen and H. Primakoff, Phys. Rev. 74, 1406 (1948); Rev. Sci. Instr. 21, 447 (1950). George W. Hinman, Carnegie Institute of Technology Report NYO-91, 1951 (unpublished), Appendix VII.

5, and 11) demonstrates the excellence of the resolution correction as applied here.

To assess the errors involved in the resolution correction, the spectrum of Re^{186} inner group in coincidence was calculated using the constants from its own line and from the Au^{198} and Cs^{137} lines (Fig. 10). The comparison, in the least favorable case, Re^{186} constants *vs* Cs^{137} constants, showed the variation in the ratio of the so-corrected spectra to be $<0.2\%$ from 150 kev to 600 kev, $<0.5\%$ up to 785 kev and to attain a maximum of 1.5% at 900 kev ($E_0=934$ kev). When the Au^{198} constants are applied to the Re^{186} spectrum, the differences are smaller.

While these differences (Cs *vs* Re constants) are invisible in the Kurie representation, they are significant in the *m* plot (spectrum correction factor) near the end point where the correction is large. The most conservative view, which we adopt, is that these differences represent the uncertainty in the resolution correction. This estimate of uncertainty may be excessive for a spectrum corrected with an internal line shape.

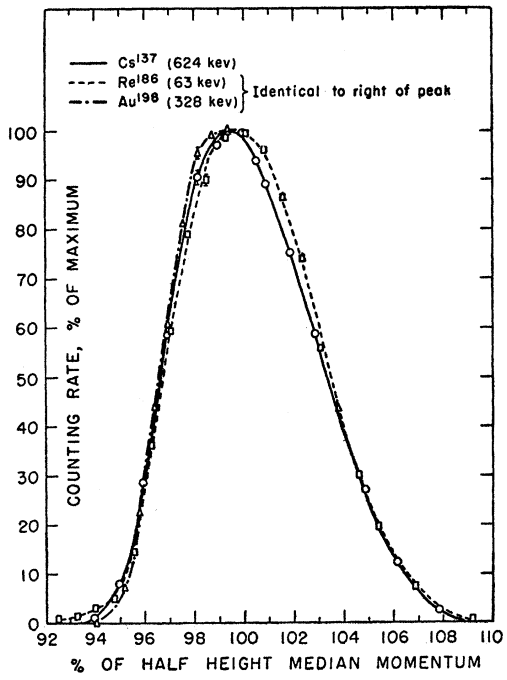

FIG. 10. Line shapes for 63 (Re^{186}), 328 (Au^{198}), and 624 (Ba^{137}) kev electrons in the 5% transmission mode of operation of the spectrometer. All sources are $\frac{1}{4}$ inch in diameter, volatilized onto 200 $\mu g/cm^2$ Al; source thicknesses were 12, 57, and 20 $\mu g/cm^2$, respectively. This comparison is taken as evidence that the line shape parameters used in the resolution correction can be considered independent of the electron energy for the samples used in the Re and Au experiments. The 624-kev line (*K*-line of the 2.5-minute 661-kev transition in Ba^{137}) was obtained free of *L*-line and the continuum of the parent Cs^{137} by counting in coincidence with *K* x-rays. Representative statistical errors near the peak are indicated. Note that the resolution correction parameters are derived from a "counting rate" plot rather than a "counting rate per unit momentum" plot.

Correction for $\beta-\gamma$ Angular Correlation

Because of the beta energy dependence of a beta-gamma angular correlation (if one exists), examination of the beta spectrum in coincidence with a gamma at a particular angle (or in a range of angles) will result in a spectrum shape which is a function of the angles employed. To obtain the shape associated with gammas at all angles (i.e., the "singles" shape, if the spectral group could be seen in singles counting not in combination with interfering beta transitions), one must apply a further correction to the observed momentum spectrum. The mathematical details of the correction and evaluation for our spectrometer are given in reference 26. For the Re^{186} spectrum in our spectrometer, the correction amounts to about -2% at 150 kev and increases to -6% at 900 kev, as the beta-gamma anisotropy increases with increasing beta energy.[25]

Inner Bremsstrahlung

Theoretical evaluations[39] of the relative number of inner bremsstrahlung (I.B.) photons per beta decay,

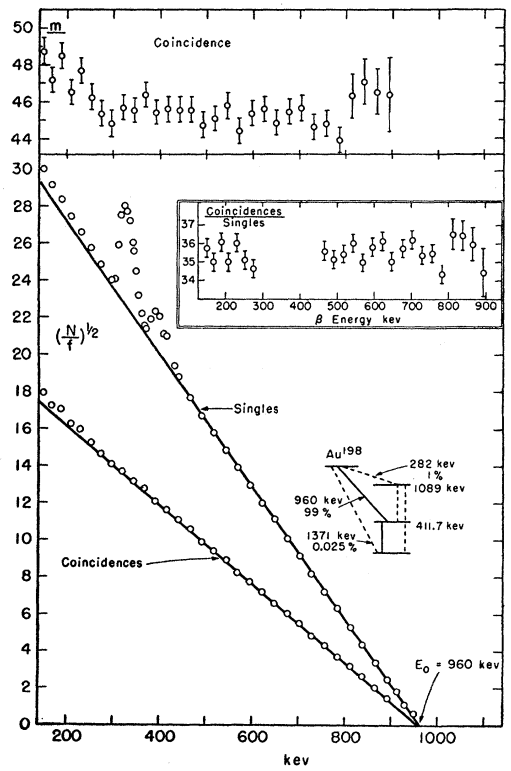

FIG. 11. Spectrum of Au^{198}. (1) Kurie plot of Au^{198} in coincidence with 412-kev gamma ray; (2) Kurie plot of Au^{198} in "singles"; (3) ratio of coincidences to singles $R/(B-bg)$ *vs* beta energy; (4) *m* function plot of Au^{198} in coincidence; (5) decay scheme of Au^{198}.

[39] C. S. Wang Chang and D. L. Falkoff, Phys. Rev. **76**, 365 (1949).

TABLE I. Summary of Au^{198} beta spectroscopy. All work on Au^{198} with reasonably thin sources, reported in the literature is listed with relevant data here. Inspection of the column "Kurie plot" with reference to the source thickness and mode of deposition used, indicates the uncertain character of the shape of the 960-kev transition below 400 kev. We have listed selected values for E_0 (Column 6) where resolutions, line shapes, and calibrations could be ascertained. Note that the 960-kev average is lower than the unselected average of 963 kev of Hollander, Perlman, and Seaborg.[a]

Reference	Source thickness (mg/cm^2) and mode of deposition	Spectrometer and estimated resolution	Region where Kurie plot is straight	E_0 (Mev) reported	E_0 (Mev) corrected by us where resolution correction and calibration are known
[b]	0.4, liquid drop	180°, 1%(?)	>200 kev	960± 5	
[c]	0.26, foil	180°, 1.5%	>600 kev[l]	966±10	
[d]	≃0.1, liquid drop	180°, 0.6%	>120 kev[m]	956± 5	960±5
[e]	0.6	lens, 4%	>250 kev	975±15	
[f]	?, liquid drop	double lens, 2%	>400 kev[n]	970±10	
[g]	?	thick lens, 5.5%	>400 kev[n]	967± 5	
[h]	0.2, foil	double lens, 0.5%	>400 kev	959± 2.5	959±2.5
[i]	?, liquid drop	180°, 1.6%	>200 kev[n]	952	962±2
[j]	0.020, volatilized	lens, 3%	>400 kev	960	961±5
[k]	0.057, volatilized	double lens, 6.7%	>400 kev		960±2
					Average E_0=960±1

[a] Hollander, Perlman, and Seaborg, Revs. Modern Phys. **25**, 469 (1953).
[b] D. Saxon, Phys. Rev. **73**, 811 (1948).
[c] P. W. Levy and E. Greuling, Phys. Rev. **75**, 819 (1949).
[d] Langer, Motz, and Price, Phys. Rev. **76**, 641 (1949).
[e] Steffen, Huber, and Humbel, Helv. Phys. Acta **22**, 167 (1949).
[f] C. Y. Fan, Phys. Rev. **87**, 252 (1952).
[g] Pohm, Lewis, Talboy, and Jensen, Phys. Rev. **95**, 1523 (1954).
[h] See reference 41.
[i] F. T. Porter, Washington University (private communication).
[j] Broyles, Thomas, and Haynes, Phys. Rev. **89**, 715 (1953).
[k] Present work.
[l] Abundant group of E_0=600 kev reported.
[m] No 282-kev group evident.
[n] Au^{199} present.

well substantiated by experiment,[40] give≈0.002 for the fraction of beta decays associated with quantum of energy $\geq W_0/10$; this fraction decreases rapidly with increasing I.B. energy. The detection of the distortion (because of I.B.) of a spectrum distribution seen in singles counting is considerably below present spectroscopic standards. However, in Re^{186} the approximately threefold more abundant ground transition will, in coincidence with I.B. of energy ≥137 kev, give rise to ≈0.008 relative contribution to the coincidence spectrum over all angles. However, a strong β-I.B. angular correlation is known,[40] such that no I.B. photons emerge at angle π to the betas, and in a lens coincidence spectrometer arrangement like ours a severe discrimination (about fivefold) against β-I.B. coincidences exists. This reduces the relative β-I.B. contribution to the coincidence spectrum to a negligible value, about 0.1%. In the case of Au^{198}, the contribution is about 0.01%.

IV. GOLD-198

An over-all test of the equipment was obtained from the coincidence spectrum of Au^{198}, under conditions as nearly as possible like those used in the Re^{186} experiment. For Au^{198}, E_0=960 kev; for Re^{186}, E_0=934 kev for the main inner group.

The abundant 960-kev beta group (see Fig. 11 for the decay scheme), which exhibits the statistical shape (see Table I for references), carries 99.0%[41] of the disintegrations to the well-studied 412-kev level in Hg^{198}. The beta—412 kev gamma coincidence data, when corrected for the coincidence efficiency (Sec. II) should exhibit a constant number of coincidences per beta recorded except for the (practically) negligible contribution to the singles count from the 0.02% ground-state transition and for the enhancement of the low-intensity 282-kev beta group in the coincidence spectrum. This latter is due to the added possibility of its detection[42] in coincidence with the 677-kev and/or 1089-kev gammas; we compute the enhancement to be ~40–50%, leading to at most a 1% increase in the coincidence count per single beta recorded at 150 kev.

The coincidence/singles ratio would also vary if other beta emitters not recorded in coincidence were present. The production of appreciable amounts of Au^{199} (E_0=460 kev, 5%; E_0=297 kev, 73%)[43] by neutron capture in Au^{198} is well known.[44] The fraction of

[40] T. B. Novey, Phys. Rev. **89**, 672 (1953); Bolgiano, Madansky, and Rasetti, Phys. Rev. **89**, 679 (1953); and K. Lidén and N. Starfelt, Phys. Rev. **97**, 419 (1955).

[41] Elliott, Preston, and Wolfson, Can. J. Phys. **32**, 153 (1954).

[42] We use reference 41 and the data of P. W. McLaughlin and G. D. O'Kelley, California Research and Development Company Report on "Counting efficiencies for sodium iodide crystal," MTA-40 (unpublished) to compute the enhancement factor for the 282-kev group of 1.4 (relative to the coincidence efficiency for the 960-kev beta group). Using the data of M. Kalkstein and J. Hollander [University of California Radiation Laboratory Report UCRL-2764 (unpublished)], we calculate an enhancement factor of 1.55.

[43] P. M. Sherk and R. D. Hill, Phys. Rev. **83**, 1097 (1951); de Shalit, Huber, and Schneider, Helv. Phys. Acta **25**, 279 (1952).

[44] R. D. Hill and J. W. Mihelich, Phys. Rev. **79**, 275 (1950); Neutron Cross Sections, Atomic Energy Commission Report AECU-2040 (Technical Information Division, Department of Commerce, Washington, D. C., 1952), Suppl. 2 (June, 1953).

Au^{199} in our samples is reduced by short, low-flux irradiation. Assuming a cross section for Au^{198} of 35 000 barns,[44] we calculate that our samples have about 0.05% of the total disintegrations as Au^{199}. The change in the ratio, coincidence/singles, due to the presence of Au^{199} (whose gamma rays are below the G threshold) is -0.1% at 150 kev.

The 6-mm diameter sources were prepared by vacuum volatilization of the neutron irradiated Au foil onto 200-$\mu g/cm^2$ Al backings. The source thickness, 57 ± 5 $\mu g/cm^2$, was obtained from the known weight of gold placed on the filament and the measured fraction of the activity collected; this was checked by an activation comparison to a weighed gold standard.

The pulse amplitude from the 411-kev gamma was artificially reduced even below that of the 137-kev gamma by inserting a perforated metal screen of about 20% light transmission between light pipe and photomultiplier while holding the other gain variables constant.[26] We believe that this would emphasize any tendency towards lower coincidence efficiency for lower gamma pulse height and thus test the over-all performance more severely. In fact the differential coincidence efficiency curve (Sec. II) applicable to the gold experiment was essentially the same as for the Re^{186} experiment.

The data are the combination of three successive spectrum "runs" the total covering a period of 24 hours. Maximum beta (B) counting rates were 65 000 per minute and the initial G rate was 135 000 per minute. Real/chance coincidence rates exceed 10/1 for every point. No β-γ angular correlation correction was necessary.[45] The data are treated as in Sec III.

Figure 11 shows the Kurie plots of the Au^{198} spectrum in coincidence and in singles and the m function plot of the coincidence spectrum. The inset gives the ratio coincidence/singles $[R/(B-bg)]$ *vs* beta energy. This ratio is seen to be constant from 150 kev to 900 kev within the statistical fluctuations of 1.5% (about 2.5% above 800 kev). The Kurie and m plots for the coincidence spectrum indicate an allowed shape to within 2% for $E_0=960\pm2$ kev over the range 300 kev to 900 kev. Note in the coincidence Kurie plot the complete suppression of the conversion lines because of the discrimination in G against the x-rays.

An upturn in the singles spectrum appears below 400 kev, amounting to about 5.5% (in the counting rate) at 180 kev, roughly $E_0/5$. [The singles spectrum taken with proportional counter detector (Fig. 5) shows the same deviations.] The coincidence Kurie plot also deviates at 180 kev by the same amount, but appears not to deviate above 300 kev. This difference (if real) is submerged in the statistical fluctuations of R in $R/(B-bg)$, and the comparison is unavailable in the range 300–400 kev due to the presence of the conversion lines in the singles spectrum; the deviations may well be identical. Such upturns may be ascribed to five effects: (1) the beta particles of Au^{199} (or other activities); (2) the 282-kev group in Au^{198}; (3) source thickness; (4) curvature of the main group in Au^{198}; or (5) an effect introduced by the apparatus.

Since Au^{199} is not counted in coincidence, it can only contribute to the singles upturn and there only to the extent of 0.05%. We have searched for other activities in this neutron-irradiated gold and found none. The relative intensity of an impurity of half-life >10 days could not have exceeded 1%. The 282-kev group in Au^{198} accounts for about 40%[46,47] of the upturn in the coincidence Kurie plot at 180 kev on the basis of the branching ratio value of 0.98% of Elliott *et al.*[41] and the enhancement factor of 1.4.[42] Cavanaugh,[47] also on the basis of gamma counting, has reported a 1.8% branching ratio for the 282-kev group which would give an apparent deviation on the Kurie plot at 180 kev of 70% of our Kurie deviation. Our source thickness was 57 $\mu g/cm^2$ uniformly deposited; this would not be expected to give an upward deviation due to source scattering of as much as 2% at 180 kev on the Kurie plot,[48] or $<40\%$ of the upturn.

Thus, ruling out Au^{199} and other impurities, we see that the deviation from the statistical shape exhibited by the coincidence and singles data for Au^{198} might be accounted for by the 282-kev group and by source thickness, taking the maximum abundance value of 1.8%[47] and the upper limit for source scattering. However, we regard this abundance of the 282-kev group as probably too high and this amount of source scattering as improbable, and believe that the deviation may not be completely accounted for in this way. The possibility that the residual upturn below 400 kev originates in an instrumental effect cannot be eliminated by the available information. On the other hand, the possibility that real curvature (of the order of 2 or 3% variation in the spectrum correction factor) may exist in the 960-kev group in Au^{198} ($\Delta I=0$, yes) cannot in our opinion be ruled out by these or any previous experiments (Table

[45] S. L. Ridgeway, Phys. Rev. **78**, 821 (1950); R. Stump and S. Frankel, Phys. Rev. **79**, 243 (1950) report no β-γ correlation for Au^{198}.

[46] In the preliminary report of this work, Porter, Freedman, Novey, and Wagner, reference 24, it was stated that all the upturn could be ascribed to the 282-kev group in Au^{198}, on the basis of Cavanaugh's[47] value for the branching and an overestimated enhancement factor of 1.75.

[47] P. F. Cavanaugh, Phys. Rev. **82**, 791 (1951).

[48] Compare, for example, the results of Langer, Motz, and Price, Phys. Rev. **77**, 798 (1950). A 50-$\mu g/cm^2$ source of Pm^{147} ($E_0=225$ kev) formed by deposition from solution exhibited a scattering deviation on the Kurie plot of about 2% at $\frac{1}{5}E_0$. Assuming that our 57-$\mu g/cm^2$ volatilized sources are at least as good as these 50-$\mu g/cm^2$ sources and that the comparison is valid at the same fraction of E_0, the 2% deviation would occur at 180 kev for Au^{198}. Actually, a smaller scattering component is anticipated for the higher energy spectrum. Further, C. S. Wu and R. P. Albert, Phys. Rev. **75**, 1107 (1949) found that 100-$\mu g/cm^2$ Cu^{64}, chemically deposited, deviates 1.5% upward in counting rates at about 115 kev, $E_0/5$, whereas Langer, Moffat, and Price, Phys. Rev. **76**, 1725 (1949) with 75-$\mu g/cm^2$ Cu^{64}, volatilized, observed no deviation at $E_0/5$.

I). The answer to this problem, which is of fundamental interest *per se*, must await experiments with much thinner samples.

In summary, the fundamental result of the Au^{198} experiments, relative to the Re^{186} experiments, is seen in the constant ratio, real coincidences/singles, as a function of beta energy above 150 kev (inset of Fig. 11), and in the closely statistical shape obtained for Au^{198} down to at least 400 kev.

V. RHENIUM-186

Inner Group Beta Transition

Some of the early beta spectroscopy[49] on Re^{186} indicated a single beta group of the allowed shape, and other early work[50] pointed to a complex beta spectrum. Metzger and Hill[20] and Steffen,[20] simultaneously discovered that the 122-kev gamma is associated with orbital capture decay to W^{186}. Both analyzed the beta spectrum into two groups with allowed shapes having end points differing by 137 kev, the energy of the gamma ray in Os^{186}. In addition, Steffen[20] obtained the beta spectrum in coincidence with the 137-kev gamma-ray, but no definite conclusions about the shape of the spectrum could be drawn from the coincidence data.

Re^{186} is conveniently produced in high specific activity by slow-neutron irradiation of natural rhenium. We irradiated $KReO_4$ as dry salt for five days at a flux of 10^{13} neutrons/cm^2 sec in the Argonne heavy water reactor, CP-5. Spectrochemical analyses on the salt set an upper limit of 1 in 10^4 for any impurity. Ten days of decay reduces the Re^{188} ($E_0=2.1$ Mev) to $<0.1\%$ of the Re^{186} activity. No beta spectroscopy on Re^{186} was done until the counting rate beyond the end point of the Re^{186} spectrum was indistinguishable from background. This also guaranteed the absence of K^{42} activity. Consideration of the products of other reactions such as (n,p), (n,α), and $(n,2n)$ indicated that only 40-day Re^{184}, 73-day W^{185}, and 117-day Ta^{182} could possibly be of concern during the beta spectroscopy (10–15 days after irradiation). The activity of a 10-millicurie sample of irradiated salt was followed for 300 days, and no trace of long-lived contamination was discernible. The decay of the sample obtained during the spectroscopy, and from separate samples followed for seven half-lives, showed only an 89-hr period.

Sources for the concidence spectroscopy were made by volatilization *in vacuo* of $KReO_4$ onto 200-μg/cm^2 Al foil. We calculate average source thickness of about 12 μg/cm^2 for the Re^{186} sources. The 6-mm diameter deposits were barely visible with strong illumination.

Figure 12 shows the pulse-height distribution from the gamma detector as it is assembled in the coincidence

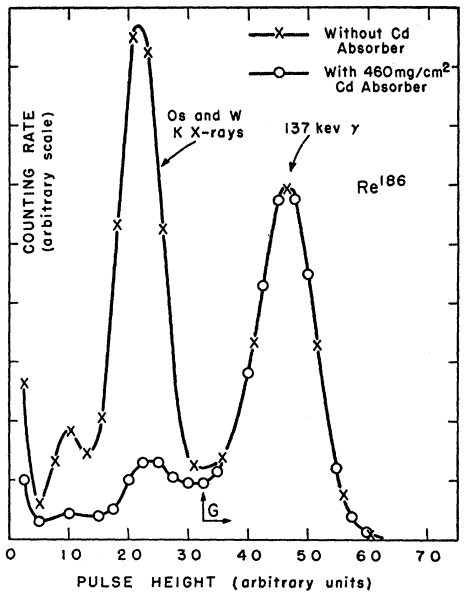

FIG. 12. Low-energy gamma pulse-height distribution from Re^{186} with the 1-inch-diameter by 24-inch-long light guide. The curves with and without 460 mg/cm^2 Cd absorber have been normalized at the 137-kev γ peak. The arrow labeled G indicates the discrimination level used in the coincidence beta spectral measurements.

source holder in the spectrometer with and without a 0.021-in. cadmium disk absorber in addition to the normal 2-mm glass vacuum seal between the source and the NaI crystal container. With this Cd absorber the over-all efficiency for the 137-kev gamma is about 1.8%. These x-rays rejected by the discrimator setting (G) are both Os (conversion) and W (conversion and electron capture) K-radiation. Including the Os K x-rays introduces the problem that the β-γ correlation must then be measured with just the same admixture of 137-kev gamma and x-rays if the spectrum is to be corrected properly. By accepting only the 137-kev gamma, we also render the G count insensitive to small drifts in the G discrimination level. The cadmium absorber was introduced so that the double coincidences due to x-β events were reduced with respect to γ-β events and hence "slow" chance events (C_S) were minimized.[26]

During the 70-hr experiments, the following items were monitored every four hours: the photomultiplier voltages; the spectrometer current control potentiometer; the fast resolving time; differential coincidence efficiency; monoenergetic beta pulse-height distribution; B background; and 137-kev photopeak amplitude. Drifts in the γ-photopeak never exceeding 3% were compensated by adjustment of the G discrimination level; no other drifts were observed. The thirty momentum values were run as a complete spectrum eight times during an experiment. Each of the eight runs was programmed so that every other point on the spectrum was taken with increasing spectrometer magnetic field

[49] See reference d of Table I and Beach, Peacock, and Wilkinson, Phys. Rev. **76**, 1585 (1949).

[50] P. J. Grant and R. Richmond, Proc. Roy. Soc. (London) **A62**, 573 (1949).

TABLE II. Beta spectrum of Re^{186}.[a,b]

		Total spectrum		Main inner group (coinc.) E_0=934.3 kev			Ground state transition E_0=1071.5 kev 76% of total betas		
1	2	3	4	5	6	7	8	9	10
E(kev)	$p(mc)$	$N_T(p)$	$(N_T/f)^{\frac{1}{2}}$	$N_C(p)$	$(N_C/f)^{\frac{1}{2}}$	$\frac{N_C}{f(E_0-E)^2}$ (×10⁵)	$N_G(p)$	$(N_G/f)^{\frac{1}{2}}$	$\frac{N_G}{f(E_0-E)^2}$ (×10⁵)
148.6	0.8159	...[c]	...[c]	915	15.29	37.87	...[c]	...[c]	...
167.9	0.8742	3461	28.47	962	15.01	38.35	2499	24.19	71.68
187.6	0.9325	3621	27.94	957	14.36	36.99	2664	23.97	73.53
208.4	0.9908	3744	27.30	1006	14.15	38.01	2738	23.34	73.15
229.6	1.0491	3848	26.65	1012	13.67	37.62	2836	22.88	73.86
251.3	1.1074	3939	26.02	1000	13.11	36.84	2939	22.48	75.12
273.8	1.1656	4007	25.33	1042	12.92	38.25	2965	21.79	74.64
296.6	1.2239	4057	24.66	1066	12.64	39.29	2991	21.17	74.64
319.8	1.2822	4076	23.90	1019	11.95	37.82	3057	20.70	75.83
343.6	1.3405	4085	23.19	1000	11.47	37.73	3085	20.15	76.67
367.6	1.3988	4061	22.44	983	11.04	37.95	3078	19.54	77.03
391.9	1.4570	4019	21.68	990	10.76	39.34	3029	18.82	76.66
416.8	1.5153	3964	20.91	932	10.14	38.40	3032	18.29	78.07
441.7	1.5736	3870	20.09	897	9.68	38.59	2973	17.61	78.21
466.9	1.6319	3772	19.32	870	9.28	39.37	2902	16.94	78.55
492.6	1.6902	3645	18.50	839	8.87	40.37	2806	16.23	78.63
518.2	1.7485	3492	17.66	778	8.34	40.16	2714	15.57	79.25
544.3	1.8067	3334	16.83	698	7.70	39.00	2636	14.97	80.60
570.4	1.8650	3154	16.05	662	7.35	40.86	2492	14.27	81.04
596.6	1.9233	2955	15.12	598	6.80	40.59	2357	13.50	80.80
623.3	1.9816	2750	14.30	541	6.34	41.61	2209	12.82	81.83
649.9	2.0399	2529	13.37	471	5.77	41.20	2058	12.06	81.88
676.6	2.0981	2306	12.49	413	5.29	42.09	1893	11.32	82.17
703.8	2.1564	2077	11.60	347	4.74	42.31	1730	10.59	82.91
730.8	2.2147	1839	10.70	286	4.22	42.98	1553	9.83	83.20
757.8	2.2730	1603	9.79	224	3.66	43.02	1379	9.08	83.73
785.3	2.3313	1371	8.88	176.7	3.19	45.79	1194	8.29	83.87
812.7	2.3896	1151	7.97	114.3	2.51	42.70	1037	7.57	85.55
840.1	2.4478	933	7.04	69.9	1.93	41.9	863	6.77	85.71
867.9	2.5061	732	6.12	37.3	1.38	43.4	695	5.97	85.9
895.5	2.5644	550	5.22	15.5	0.88	51.0	534	5.14	85.2
915.9	2.6039	444	4.62				444	4.62	87.2
934.5	2.6429	347	4.04				347	4.04	85.7
945.8	2.6664	303	3.75				303	3.75	87.8
957.0	2.6899	254	3.41				254	3.41	87.6
968.3	2.7134	211	3.09				211	3.09	88.4
979.6	2.7368	165	2.71				165	2.71	86.0
990.8	2.7601	133	2.42				133	2.42	88.4
1001.9	2.7833	97.8	2.06				97.8	2.06	86.5
1013.1	2.8065	71.8	1.75				71.8	1.75	88.9
1024.2	2.8296	46.2	1.40				46.2	1.40	86.1
1035.3	2.8526	27.6	1.07				27.6	1.07	86.6
1046.4	2.8757	13.5	0.75				13.5	0.75	87.2
1057.7	2.8988	5.2	0.46				5.2	0.46	110.3

[a] Columns 3 and 4 give the total (singles) momentum distribution and Kurie representation. Columns 5, 6, and 7 give the momentum distribution, Kurie representation, and m function for the main inner group in coincidence with 137-kev gamma. Columns 8, 9, and 10 give the analogous data for the ground state transition, computed using a relative abundance of 76% of total betas.

[b] The data are normalized such that $N_T=N_C+N_G$. Actual experimental data (not smooth curve values) are given. The Fermi function f is corrected for orbital electron screening. [National Bureau of Standards Applied Mathematics Series 13 (1952). We use the "K binding energy data" curve of Fig. 13 therein.] Energy values are from J. L. Wolfson and H. S. Gellman [Chalk River Report PD-255 (unpublished)].

[c] "M" line of 137.2-kev gamma present.

and the remaining points with decreasing field. This procedure was adopted so that the final data would reflect no short- or long-term instrumental drifts or hysteresis effects of any kind. The maximum B rate and G rate maintained dead-time losses at less than 1%. Between 4000 and 6000 coincidences were accumulated at each point below 840 kev, decreasing to 750 coincidences at 895 kev, the highest energy recorded. Real to chance ratios exceeded 10 below 760 kev, and dropped to 2 at 895 kev. Values of R/R' ranged between 1.010 and 0.994 (see Sec. III). As a check on the statistical reliability of the data, the eight values of $R/(G-bg)$ at each momentum value were examined for trends and abnormal fluctuations. Applying standard criteria, we found that the distribution was perfectly normal (Gaussian) and exhibited no trends; only 2% of the values deviated from the average by more than twice the standard error and none by more than 2.5 times.

The beta spectrum in coincidence with the 137-kev gamma is given in Table II, columns 5 and 6. The data have been treated as noted in Sec. III with the spectrometer resolution correction applied and with correction for β-γ directional correlation made. The β-γ correlation as a function of beta energy is shown in

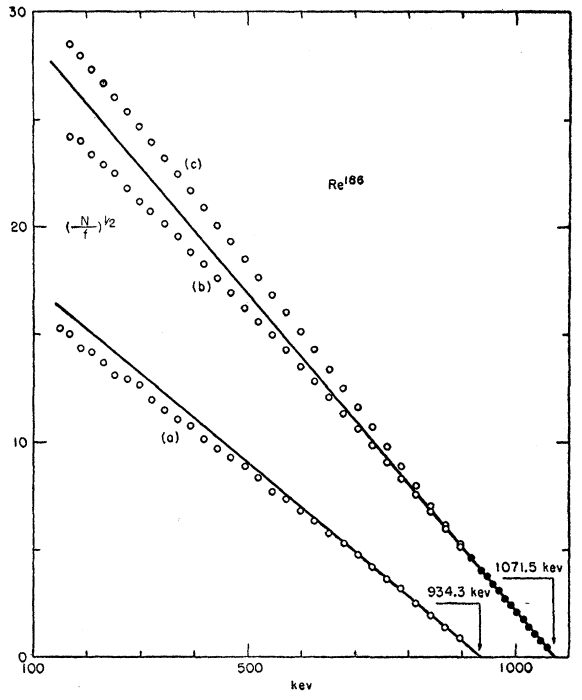

FIG. 13. Kurie plots of Re^{186}. Data in Table II. Curve (a), main inner group in coincidence with 137-kev gamma ray. Curve (b), ground-state transition by subtraction of (a) from (c) assuming ground-state transition abundance of 76% of total betas. Curve (c), total singles spectrum. Solid circle points obtained from another experiment (E_0 measurement) and normalized.

Fig. 3(e) of reference 25.[51] Actual experimental values (not smooth curve) are tabulated. The conventional uncorrected Kurie plot is shown in Fig. 13(a). The plot does not have the allowed shape, nor does it exhibit the unique "α" shape (associated with $\Delta I=2$, yes).

The character and quantitative measure of the deviation from the allowed shape is best discussed in terms of the plot (Fig. 14) of the experimental values $N/[f(E_0-E)^2]=m$, the experimental (shape) correction factor. The maximum beta energy E_0 as read from the "allowed" Kurie plot is 933.5±3.0 kev. The experimental correction factor m is sensitive to the value of E_0 for E near E_0. In another experiment, to be described below, we have narrowed the limits of experimental error, obtaining $E_0=934.3\pm1.3$ kev. The experimental points have been computed with this value for E_0, and

[51] Reference to Fig. 3(e), reference 25 will disclose that the β–γ angular correlation curve used to correct the spectrometer coincidence data differs from the final best evaluation of this function. The curve used was based on earlier measurements. The lengthy computations of the spectrum shape and the theoretical fittings thereto were not repeated when the better data on the β-γ correlation became available. The difference in the m function of the inner group of Re^{186}, as corrected with the final β-γ anisotropy, would be very small, about 0.5% reduction in the maximum span of m (Fig. 14). This recorrection would actually slightly improve the fit of the experimental m function with the theoretical curves (Fig. 18). The effect on the ground state m function is of still lesser importance, because of the relative branching ratios.

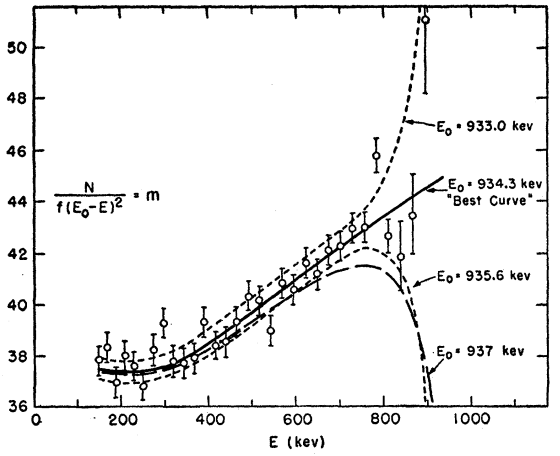

FIG. 14. Experimental spectrum correction factor (m) for Re^{186} inner group in coincidence. Solid curve presents best fit to data. Data in Table II. Curves labeled 933.0 kev and 935.6 kev give estimated upper and lower limits between which true m function is judged to lie. Curve labeled 937 kev indicates that the m function cannot be made constant even for a higher E_0 value.

are given in column 7, Table II. The solid curve of Fig. 14 gives the estimated best fit to these points.

The error flags in Fig. 14 show the statistical counting error ($T^{\frac{1}{2}}/R$), only. The two dashed curves labeled $E_0=933.0$ kev and $E_0=935.6$ kev give our estimates of the safe limits of error. The m function is, we believe, established within the accuracy represented by the error band between these two curves. The total error is computed taking account of the errors[26] in: (1) the E_0 value, 934.3±1.3 kev; (2) the resolution correction; (3) β-γ directional correlation correction; (4) the approximately 5% error in $2\tau_f$; and (5) reasonable statistical limits. The individual contributions (% of m) to the total error in m are shown in Fig. 15, together with the total error, as a function of energy.

The variation in the experimental correction factor m (solid curve) is about 18% from 150–934 kev.

The experimental points, even taking into account the net uncertainty in the data, seem to demand the indicated curvature (solid curve) in the region from 150 to 300 kev. Consideration of relative abundances shows that this trend cannot be due to the 307-kev group in Re^{186}. Such a rise towards low energy is not readily attributable either to source thickness effects in the approximately 12-μg/cm^2 sources used, or to contaminant activities detected in coincidence. As will be shown in the m plot (Fig. 16) for the ground state transition its experimental shape correction factor is, in contrast, linear in this region. We believe this to be a real difference between the two spectra. However, we note that the evidence presented from the spectra of Au^{198} and P^{32} (see Secs. II and IV) does not rule out the possibility that purely instrumental effects, e.g., scattering from the coincidence source holder, as distinguished from source thickness effects may contribute upturns of 1–2% around 300 kev.

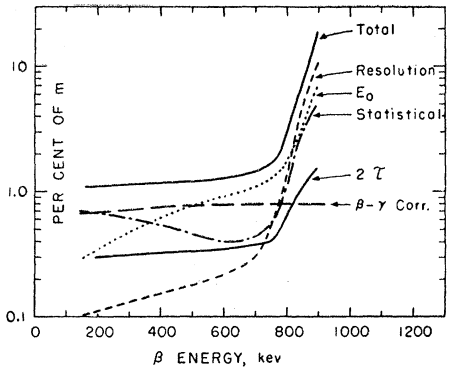

FIG. 15. Experimental errors in Re^{186} inner group m plots as a function of beta energy (individual and total). Total error curve used in computing error band limiting curves in Fig. 14.

As has been emphasized the results are critically dependent on the relative coincidence efficiency as a function of β energy for the particular combination of detectors and circuits employed. Our measurements showed that inclusion of the correction for the small variation of the relative coincidence efficiency (Fig. 8) actually did not materially affect the shape of the coincidence spectrum for the scintillation counter.

During the course of the present work, Koerts[52] examined the beta spectrum in coincidence with the 137-kev gamma and found it to have the allowed shape, not in agreement with the present work. The reasons for the disparity in the experimental results are not evident.

Composite Beta Spectrum

The singles or total beta spectrum is recorded at the same time as the coincidence data; it is just $[(B^*/\eta)-bg]$; η is the singles efficiency. For the measured total beta momentum distribution $M(p)=e^{\lambda t}[(B^*/\eta)-bg]/p$, one needs accurate values for the decay constant λ. Our experiments[26] give 88.9±0.2 hours for the Re^{186} half-life, based on 30 points on the momentum spectrum and on external samples followed for 300 hours.

The conventional Kurie plot (Fig. 13, curve c) clearly demonstrates a definite continuous curvature concave towards the energy axis. The identical curvature (within 1%) was obtained with the proportional counter. This curvature furnished what is probably the strongest evidence that one or both components are curved concave downwards, in the opposite sense to the curvatures usually ascribed to effects such as scattering and source thickness. The Au^{198} and P^{32} spectra demonstrate the absence of instrumentally introduced curvature above 400 kev, and certainly of any downward curvature even below 400 kev. The points from the experiment described above are represented by circles (Fig. 13, curve c). The statistical error in these points is everywhere small compared to the size of the circle. The resolution correction to the singles data is smaller than that applied to the coincidence data in the neighborhood of 900 kev, since the singles spectrum extends to higher energies. However the resolution correction is too large in the region of the end point to obtain the requisite accuracy in the end-point measurement using the high-transmission mode of operation of the spectrometer.

Determination of Transition Energies[26]

For a determination of E_0 for the ground-state transition, a 3-mm diameter, 30 $\mu g/cm^2$ thick volatilized Re source on 200-$\mu g/cm^2$ Al foil was prepared. The Re^{188} content was carefully checked and the sample was allowed to decay for 14 days until the calculated Re^{188}/Re^{186} was 0.005% and the count 160 kev beyond the Re^{186} end point was indistinguishable from background (9 counts/min). The spectrometer was adjusted to give 0.8% transmission and 2.0% resolution and the proportional counter beta detector was used.

Calibration of the reference line in the Re^{186} source was accomplished in a separate experiment with a mixed Re^{186}-Au^{198} source.[53] The source for the calibration experiment (1.5-mm diameter, about 150 $\mu g/cm^2$ total thickness) was prepared by volatilizing Au^{198} (about 130 $\mu g/cm^2$) onto 200-$\mu g/cm^2$ Al foil, and without moving the foil or mask in the volatilization apparatus, volatilizing Re^{186} (<20 $\mu g/cm^2$) over the gold. The observed resolutions were 1.27(±0.02)% for the Au^{198} K-line (328 kev) and 1.30(±0.03)% for the 63-kev Re^{186} K-line, and no evidence for tailing out or scattering was visible in the line profiles. The $H\rho$ value obtained for the Re^{186} K-line from the comparison is 874.40±0.41 $H\rho$. Using the Cauchois and Hulubei value for the K binding energy of Os, 73.87 kev, as computed by Slack,[54] we obtain for the energy of the first excited state in Os^{186}, 137.19±0.07 kev. Day has measured the energy of the gamma ray on a Cauchois bent-crystal spectrometer,[55] obtaining 137.19±0.12 kev.

Using the value obtained for the $H\rho$ of the line, applying resolution and decay corrections, and a carefully determined value for the counter background, we calculated the conventional Kurie plot. No deviation from linearity could be seen from 935 kev to E_0 on a very expanded plot. The points extended to within 1.5%

[52] L. Koerts, Phys. Rev. **95**, 1358 (1954). The large abundance of the ~300-kev group reported by Koerts suggests the presence of an effect which may mask the small downward curvature which we find.

[53] The standard K-line momentum in Au^{198} was taken as 2222.4 ±0.4 gauss cm. The gamma-ray energy is quoted to somewhat better precision; Muller, Hoyt, Klein, and DuMond, Phys. Rev. **88**, 775 (1952). However, the uncertainty in the K binding energy of Hg limits the accuracy of the calculated conversion line to about the same limits as those quoted for the direct measurement of the $H\rho$ of the conversion line by D. A. Lind and A. Hedgran, Arkiv. Fysik. **5**, 29 (1952).

[54] L. Slack (privately circulated tables).

[55] P. Day, Phys. Rev. **97**, 689 (1955). *Note added in proof.*—N. Ryde and B. Anderson, Proc. Phys. Soc. (London) **B68**, 1117 (1955), obtained 137.22±0.03 kev for this gamma on a crystal spectrometer.

of the end point; for the last point the resolution correction was about 15%, and at 4% below the end point, about 4%. The data for this experiment, normalized to that of the high-transmission singles experiment over the range 730–935 kev, are shown as solid circles on Fig. 13, curves b and c. The normalizing factor obtained by comparison of the data from the low- and high-resolution modes of operation of the spectrometer showed a mean deviation of 0.2% over this range, and no evidence of a trend.

Graphical determination on an expanded plot and an unweighted least squares calculation gave $E_0=1071.5 \pm 1.3$ kev, including estimated contributions to the error from the uncertainties of the Au^{198} standard and from the calibration procedure. From the gamma energy of 137.19 ± 0.07 kev the energy of the main inner group is computed to be $E_0=934.3\pm1.3$ kev, in comparison to the observed 933.5 ± 3.0 kev.

Ground-State Beta Transition

By subtracting the inner group spectrum from the singles data, with an appropriate normalization to take account of the beta branching ratio, the shape of the ground-to-ground beta distribution can be obtained.

The branching ratio was obtained to the requisite accuracy (1% in ~25%) from the beta spectrometer coincidence data along with the known efficiencies for counting betas and gammas. The following equation is employed:

$$\frac{\beta^-(934)}{\beta^-(934)+\beta^-(1071)}=\frac{(G/\epsilon_\gamma)+(e^-/\epsilon_\beta)}{(1/\epsilon_\beta)\int_0^{p_{max}}(B/\Delta p)dp},$$

where B and G are the beta and analyzed 137-kev gamma photopeak counts recorded in the spectrometer (corrected for dead-time losses and decay) at efficiencies ϵ_β and ϵ_γ, respectively, and e^- is the total $K+L+M$ conversion line area. Δp is the "resolution width" of the spectrometer.[26] ϵ_β was obtained by counting an absolutely standardized Ba^{137m} source in the spectrometer, and ϵ_γ was computed from the source-crystal geometry, taking account of absorption and edge effects[42] in the crystal. G is corrected for the presence of about 10% of 122-kev gamma counts in the photopeak. We obtain for the inner group a branching ratio of $23.4(\pm1.5)$%, and for the ground state $76.6(\pm1.5)$% of total betas, and use the value 76% in further discussion.

Curve (b), Fig. 13, shows the Kurie plot of the ground state beta transition obtained by subtraction of the inner group from the composite spectrum using a multiplying factor which yields the 76% branching ratio. This factor is obtained by trial and error comparison of the areas of the momentum spectra. This Kurie plot is very similar in shape to that of the inner group, being concave downward toward the energy axis. In

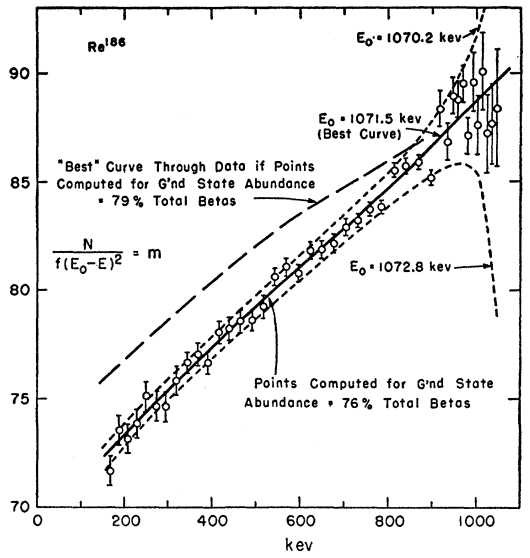

FIG. 16. Experimental spectrum correction factor (m) for Re^{186} ground-state transition. $E_0=1071.5$ kev. Solid curve presents best fit to data. Curves labeled 1070 kev and 1073 kev give estimated upper and lower limits between which true m function is judged to lie, for a branching ratio of 76% of total betas. Curve labeled "79%" represents best fit to data (experimental points not shown) for a branching ratio of 79% of total betas. Data in Table II.

Fig. 16, the m plot for the ground-state transition, we indicate by dashed curves labeled $E_0=1072.8$ kev, and $E_0=1070.2$ kev, as in the m plot of the inner group (Fig. 14), the extremes of the "safe" error band for the ground transition. These take into account the uncertainty in E_0, the uncertainties in the resolution correction of the total spectrum, the assigned uncertainty in the inner group, and reasonable upper and lower limits consistent with the statistical uncertainties of the counts. In computing the error limits, we have arbitrarily ignored the contribution to the total error due to the uncertainty in the branching ratio. In Table II, columns 8–10, we present the relevant data on the ground transition. The values listed are the actual experimental numbers (not smooth curve). The variation in the m function for the ground-state transition is about 23% from 150 kev to E_0.

Conventional Subtraction Analysis

The disparity between the results of Guss, Killion, and Porter[22] (in which an "α" shape was found for the inner group on subtraction of an allowed shape for ground state group) and the allowed shape found by other investigators[20,52] was checked by application of the same procedure to our total singles data. The result[26] of subtracting the least square allowed shape fit to the high-energy end (>934 kev) of the singles spectrum is an inner group shape which is indeed, accidently, a fair approximation to the $C_{1T}^{(2)}$ correction factor. Close examination of the curve discloses only a very slight

TABLE III. Subsidiary data obtained on the nuclear decay of Re^{186}.

(1)	$e_K^-(137)/[\beta^-(934)+\beta^-(1071)]=0.042_8$	
(2)	$e_L^-(137)/[\beta^-(934)+\beta^-(1071)]=0.065_7$	
(3)	$e_L^-(137)/e_M^-(137)$[a]$=5$	
(4)	$e_K^-(122)/[\beta^-(934)+\beta^-(1071)]=0.0042_9$	
(5)	$e_L^-(122)/[\beta^-(934)+\beta^-(1071)]=0.0059_5$	
(6)	$e_L^-(122)/e_M^-(122)$[a]$=5$	
(7)	$\beta^-(934)/[\beta^-(934)+\beta^-(1071)]=0.24\pm0.015$	
(8)	K x-rays (W)/K x-rays (Os)[b]$=1.9$	
(9)	$\gamma_{627}/\gamma_{137}=0.0070$	
(10)	$\gamma_{764}/\gamma_{137}=0.0034$	
(11)	$E_\gamma=764$ kev[c]	
(12)	Electron capture[d] [total L/K]$=0.18$	
(13)	$e_K^-(137)/e_K^-(122)=10.0$	
(14)	$\gamma(137)/\gamma(122)$[a]$=9$	
(15)	$[e_{K+L+M}^-(122)/\gamma(122)]/[e_{K+L+M}^-(137)/\gamma(137)]\approx1$ [estimated from (13) and (14).]	
(16)	K x-rays/K vacancies (Os and W)[e]$=0.93$	
(17)	From (1), (2), (3)	$K/L/M(137)=0.65/1/0.2$
(18)	From (4), (5), (6)	$K/L/M(122)=0.72/1/0.2$
(19)	From (1), (2), (3), (7), (9)	$\alpha_K(137)=0.36_4$
(20)	From (1), (2), (3), (7), (9)	$\alpha_L(137)=0.53_7$
(21)	From (7), (8), (12), (15), (16)	E.C. to ground/decay$=0.063$
(22)	From (7), (8), (12), (15), (16)	E.C. to 122 kev level/decay$=0.021$
(23)	From (7), (8), (12), (15), (16)	β^-(934 kev)/decay$=0.22\pm0.02$
(24)	From (7), (8), (12), (15), (16)	β^-(1071 kev)/decay$=0.70\pm0.02$
(25)	From (7), (8), (12), (15), (16)	β^-(307 kev)/decay$=0.0010$
(26)	From (7), (8), (12), (15), (16), (10)	γ_{764}/decay$=0.00034$
(27)	From (7), (8), (9), (12), (15), (16)	γ_{627}/decay$=0.00070$
(28)		$E_0\beta_1=1071.5\pm1.3$ kev
(29)		$E_0\beta_2=934.3\pm1.3$ kev
(30)	From (28) and (11)	$E_0\beta_3=307$ kev
(31)		$E(\gamma_1)=137.19\pm0.07$ kev
(32)		$E(\gamma_2)=122.67\pm0.21$ kev
(33)		Half-life$=88.9\pm0.2$ hr
(34)	Curves and nomographs of S. Moszkowski[f]	log $f_0t(\beta934)=8.00$
(35)	Curves and nomographs of S. Moszkowski[f]	log $f_0t(\beta1071)=7.68$
(36)	Curves and nomographs of S. Moszkowski[f]	log $f_0t(\beta307)=8.95$
(37)		Upper limit β^+/decay$=2\times10^{-6}$

[a] See reference 20.
[b] Paul Day, Cauchois spectrometer (private communication).
[c] See Metzger and Hill, reference 20.
[d] H. Brysk and M. E. Rose, Oak Ridge National Laboratory Report ORNL-1830 (unpublished).
[e] Broyles, Thomas, and Haynes, Phys. Rev. **89**, 715 (1953).
[f] S. Moszkowski, Phys. Rev. **82**, 35 (1951).

deviation over the mid energy range, but a fairly sharp drop off below the $C_{1T}^{(2)}$ shape below 400 kev, for an E_0 value of 915 kev, 19 kev too low.

Additional Data on Re^{186}

As the relative intensity of the 307-kev beta group is of concern in connection with the aforementioned curvature in the coincidence spectrum near 200 kev, a measurement of the intensity of gammas following the 307-kev beta was made. Standard scintillation spectrometry techniques[26] were used to compare the areas of the 764- and 627-kev photopeaks to that of the 137-kev gamma. The ratio (627-kev γ/764-kev γ) obtained was 1.95 ± 0.17. The ratio (627-kev γ/137-kev γ) $=7.0\times10^{-3}$, leading to a 307-kev β-per total beta intensity of $0.105(\pm0.03)\%$ (if the conversion of the 627- and 764-kev gammas is neglected).

We present here (Table III) a summary of data on the decay of Re^{186}, including a number of values obtained incidental to the spectrum shape studies. We list first in Eqs. (1) to (16) the primary experimental quantities (from the present experiment unless otherwise indicated) and theoretical quantities needed for the calculations.

It will be noted from Table III that the values agree well with those of Metzger and Hill[20] and Steffen[20] except for the quantities (21) and (22) where the agreement is better with Steffen and for the quantities (25), (26), and (27) where they favor the results of Robinson, Whittle, and Jastram.[56]

VI. THEORETICAL INTERPRETATIONS OF BETA SPECTRAL SHAPES OF Re^{186}

From the ft values of the two main beta transitions the spectra are classified as first forbidden; the shell model prediction of the Re^{186} ground state parity (odd), together with the even parities of the ground and first excited states in Os^{186}, support the first forbidden character of the transitions. The nonunique shapes found for both transitions justify the assignment of a $1(-)$ character to the ground state of Re^{186}. (Either $0-$ or $2-$ assignments would require an "α" transition

[56] Robinson, Whittle, and Jastram, Phys. Rev. **91**, 498(A) (1953).

for one or the other beta groups.) From the parametric fitting of these beta distributions to theoretical spectral shapes, values of ratios of nuclear matrix elements are obtained. From the similar fitting to theory of the directional correlation of inner group beta and 137-kev gamma, independent values for the same nuclear matrix element ratios governing the beta transition were derived[25]; these results are compared in Sec. VII.

The experimental correction factors used in the fittings are the solid curves of Figs. 14 and 16.

We calculate theoretical correction factors[57] for both ground-state and main inner group transitions involving the combination of scalar and tensor interactions only, $G_S S+G_T T$. This choice is based on the weight of current evidence[58] that these two interactions contribute to the beta process rather than the VA combination[59] and that the pseudoscalar invariant has not been found necessary[2-4] in the fitting of the spectrum of RaE, which is judged also to be a $\Delta I=1$, yes transition.

From Konopinski and Uhlenbeck[57] we obtain the direct terms, and from Pursey[60] the cross terms, for the spectrum correction factor for a transition with spin change one with a parity change.

Following Lee-Whiting[4] we define ratios

$$x=i\frac{G_S}{G_T}\frac{\int\beta\mathbf{r}}{\int\beta\boldsymbol{\sigma}\times\mathbf{r}},\qquad \Lambda=\frac{2\rho}{\alpha Z}\frac{\int\beta\boldsymbol{\alpha}}{\int\beta\boldsymbol{\sigma}\times\mathbf{r}};\tag{2}$$

$\rho=$nuclear radius. We equate[61] $\rho=\frac{1}{2}\alpha(\hbar/mc)A^{\frac{1}{3}}$ cm, as do Rose *et al.*[62] $\rho=1.41\times10^{-13}A^{\frac{1}{3}}$ cm for $\alpha=1/137.00$.

For the inner group, the B_{ij} matrix element also contributes to the beta process (but not for the ground-state[63] decay). Inclusion of B_{ij} would add a third nuclear matrix element ratio parameter to the fitting procedure. Justification for avoiding this complication is derived from consideration of the about tenfold higher ft values for unique ($\Delta I=2$, yes) transitions which depend only on B_{ij}. While we recognize that the B_{ij} term contribution may be significant, we are able to match the theoretical and experimental shape factors for the inner group without it. By extension of the same argument, we omit the third forbidden matrix elements.[2]

Following Yamada[2] and Lee-Whiting,[4] we effect a transformation of the parameters such that if complete cancellation of the largest energy-independent terms ($\propto\rho^{-2}$) occurs (in the expansions of L_0, M_0, N_0 and L_1, the conventional combinations of the electronic radial wave functions), then the new parameter vanishes. In terms of the new parameter, y, the total ρ^{-2} term becomes $(y^2/\rho^2)[\alpha^2Z^2/2(1+S)]$, where

$$y=\tfrac{1}{2}(1+S)\Lambda-1-x,\tag{3}$$

and $S=(1-\alpha^2Z^2)^{\frac{1}{2}}$.

As Yamada[2] has shown, this transformation also causes the smaller terms proportional to ρ^{-1} to vanish as y vanishes; i.e., in the resulting correction factor, erms in ρ^{-2} and in ρ^{-1} are eliminated *explicitly*.

Taking the coupling constants[64] and the quantities x and Λ[65] as real, we can write

$$C_{1ST^{(1)}}=\left(\frac{G_S{}^2}{x^2}\right)\left|\int\beta\mathbf{r}\right|^2\left(\frac{2}{1+S}\right)\left(\frac{\alpha Z}{2\rho}\right)^2U,\tag{4}$$

where the energy-dependent (shape-determining) terms are confined to

$$\begin{aligned}U=&y^2[2L_0/(1+S)]\\&+xy\{[4L_0/(1+S)]+2\zeta(\tfrac{1}{3}KL_0+N_0)\}\\&+x^2\{[\tfrac{1}{2}\zeta^2(1+S)](\tfrac{1}{3}K^2L_0+2L_1+M_0+\tfrac{2}{3}KN_0)\\&+[2L_0/(1+S)]+2\zeta(\tfrac{1}{3}KL_0+N_0)\}\\&+y[4L_0/(1+S)-2\zeta(\tfrac{1}{3}KL_0-N_0)]\\&+x[4L_0/(1+S)+4\zeta N_0-\zeta^2(1+S)(L_1-M_0)]\\&+\{[\tfrac{1}{2}\zeta^2(1+S)](\tfrac{1}{6}K^2L_0+\tfrac{1}{2}L_1+M_0-\tfrac{2}{3}KN_0)\\&\qquad-2\zeta(\tfrac{1}{3}KL_0-N_0)+2L_0/(1+S)\},\end{aligned}\tag{5}$$

where $K=W_0-W$ and $\zeta=2\rho/\alpha Z=0.07511$ for Os^{186}.

For values of the parameters x and y for which the energy dependence of U is significant (y small), the six terms of Eq. (5) in powers of x and y do not suffer severe mutual cancellation in computing U. However, in evaluating the six coefficients of these terms, in all except the y^2 term, one finds that the coefficients represent very small differences between the quantities involved. To retain, say, 2-figure accuracy in the coefficients requires that at least 5 significant figures be employed in evaluating the L_0, M_0, and N_0 functions. The advantage of transformation (3) is then that fewer

[57] See E. J. Konopinski and G. E. Uhlenbeck, Phys. Rev. **60**, 308 (1941) for definition and notation.

[58] E. J. Konopinski and L. M. Langer, in *Annual Reviews of Nuclear Science* (Annual Reviews, Inc., Stanford, 1953), Vol. 2, p. 261.

[59] B. M. Rustad and S. L. Ruby, Phys. Rev. **97**, 991 (1955) show that the tensor predominates over the axial vector.

[60] D. L. Pursey, Phil. Mag. **42**, 1193 (1951).

[61] We have not investigated the sensitivity of the fitting to the choice of ρ value. Lee-Whiting[4] has stated that the fitting is fairly insensitive for RaE over a factor of two variation in ρ. However, in the fitting of the second forbidden ground-state transition in Cs^{137}, the possibility of obtaining a fit at all is dependent on the selection of a value for $\rho\approx1.2\times10^{-13}A^{\frac{1}{3}}$ cm instead of $\rho\approx1.4\times10^{-13}A^{\frac{1}{3}}$ cm. [M. Freedman (unpublished).]

[62] Rose, Perry, and Dismuke, Oak Ridge National Laboratory Report ORNL-1459, 1953 (unpublished).

[63] $B_{ij}=0$ for $I=1\leftrightarrow I=0$ transitions.

[64] L. C. Biedenharn and M. E. Rose, Phys. Rev. **83**, 459 (1951).

[65] C. L. Longmire and A. M. L. Messiah, Phys. Rev. **83**, 464 (1951).

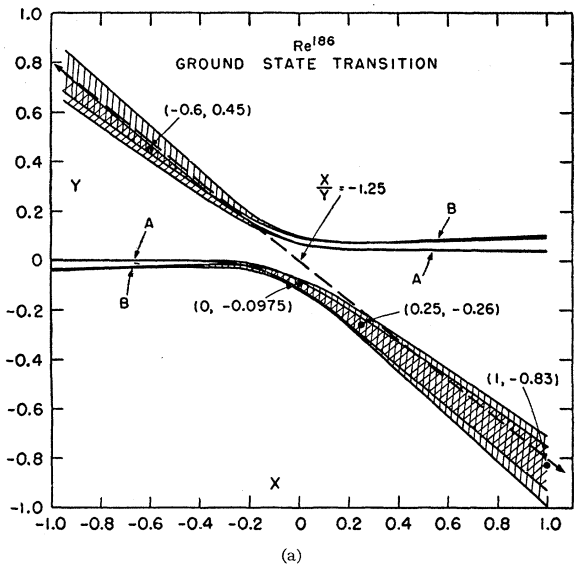

(a)

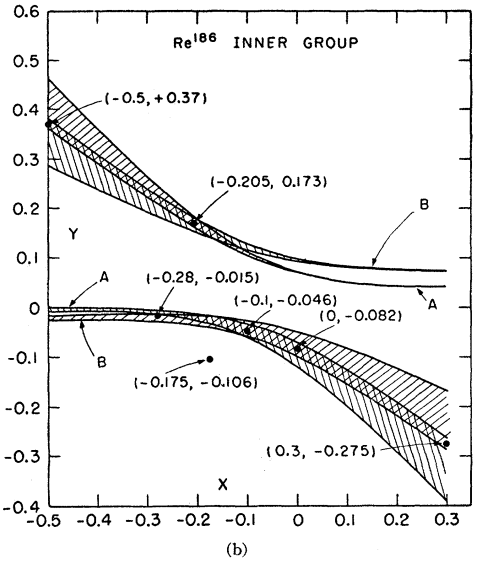

(b)

FIG. 17. Quadratics in x and y for which theory reproduces ratio of experimental shape correction factor at two energies (Eq. 6). Because of experimental uncertainty, band (hatched) is generated rather than single conic section. Figure 17(a) is for the inner group and 17(b) is for the ground state transition in Re^{186}. Experimental ratios are taken at ($p=1.2\ mc$, $p=1.8\ mc$) for bands A and at ($p=1.8\ mc$, $p=2.4\ mc$) for bands B. All conics are hyperbolas. Points (x,y) in cross-hatched region may produce good fits to the experimental shape correction factor. Theoretical correction factors are displayed in Figs. 18 and 19 for the indicated points.

figures need be carried through the rest of the computation. To obtain 5 significant figures in the L_0, M_0, and N_0, one must retain higher order terms in the expansion of the L_0, M_0, and N_0 functions in powers of ρ. This has been called "taking account of the finite de Broglie wavelength of the electron in comparison to the nuclear radius."[2,66] L_0 and N_0 are given in Yamada,[2] Eqs. (1) and (2), and M_0 in Konopinski and Uhlenbeck.[57] We use the first three terms in each expansion, so that Eq. (5) is complete to terms in ρ^2 and contains some terms in ρ^3 and ρ^4. L_0 and M_0 so computed are valid to 5 figures and N_0 to 4 or 5. We obtain the relatively small quantity L_1 by graphical interpolation from the table of Rose, Perry, and Dismuke.[62] Unfortunately, these 4-figure tables do not quite carry enough significant figures for L_0, M_0, and N_0.

Expression (4) is identical to Lee-Whiting's Eq. (1) if in evaluating U we keep only terms through ρ^2.

The expansions of the electronic radial wave function combinations L_0, M_0, and N_0 near the nuclear surface are given for the Coulomb field case only, i.e., the nuclear charge is considered to be concentrated at the center of the nucleus. Rose and Holmes[67] have shown how sensitive the L_0, M_0, and N_0 functions are to changes in the charge distributions. For example, the assumption of a uniform charge distribution leads to about 50% alteration in M_0. In view of the lack of a well established model for the nuclear charge distribution, it appears that one cannot take account of this effect of finite nuclear size with the necessary accuracy. Two arguments may be adduced to justify the utility of precise calculations based on the unrealistic point charge model which surely yields grossly erroneous wave function combinations, in comparison to the stated requirements of precision. Yamada[2] argued that in the case of RaE the parameter values for which a fit was obtained were not sensitive to the nature of the nuclear charge distribution, as anticipated theoretically for cases, such as RaE, where extensive deviation from the allowed shape indicates near-cancellation of the large energy-independent terms, the ones most sensitive to the detailed nature of the charge distribution. We cannot with certainty apply the argument to the case of Re^{186} where the deviation from the allowed shape is slight. However, as we also compute[25] the nuclear parameters x and y by fitting the experimental differential β-γ directional correlation assuming point nuclear charge, a comparison of the fittings may be useful even if the absolute magnitudes of the parameters derived from either are not accurate.

The ratio of the values of the experimental correction factor, m, at two energies, E_i and E_j, can be reproduced for a set of (x,y) values by the theoretical expression (5); i.e.,

$$m_i/m_j=[U_i(x,y)]/[U_j(x,y)]. \qquad (6)$$

This set generates a conic section in the x,y plane. Several pairs of points on the experimental correction factor are chosen and the conic section generated by each pair is plotted. Since actually the experimental correction factor has uncertainty, each pair of energy values determines a range for the correction factor ratio; thus a band rather than a single conic is obtained. The

[66] M. E. Rose and C. L. Perry, Phys. Rev. **90**, 479 (1953).

[67] M. E. Rose and D. K. Holmes, Phys. Rev. **83**, 190 (1951).

range used was restricted to within the "safe" error limits of Figs. 14 and 16. It is in the common area of the bands that values of x and y lie which *may* produce fits to the experimental correction factor over the entire energy range. Figures 17(a) and 17(b) show these conic section plots for the inner group of Re^{186} and the ground-state transition respectively. Two hatched conic section bands are shown in each figure; for band A, i and j of Eq. (6) correspond to $p_i=1.2$ and $p_j=1.8$ mc and for band B, $p_i=1.8$ mc and $p_j=2.4$ mc. These bounding curves are all hyperbolas. In the computation of the theoretical correction factors $U(x,y)$, we have used only the "best" E_0 values, 934.3 kev and 1071.5 kev, respectively.

Not all the points (x,y) in overlap regions (cross-hatched) of Fig. 17 are expected to be equally good in fitting the entire spectrum, since all the details of the experimental correction factor are not contained in the points chosen for the conic section plots. With selected values of x,y from Fig. 17 (indicated points) the theoretical correction factor was calculated from (5) and compared in Fig. 18 to the experimental data for the inner group and in Fig. 19 for the ground-state transition. Experimental and theoretical curves are normalized at 541.2 kev ($p=1.8$ mc). Each heavy solid curve in Fig. 18 or 19 is a reproduction of the solid curve in Fig. 14 or 16 respectively. In Fig. 18, one experimental curve is shifted vertically by 3.6 ordinate units and one by 7.2 units for clarity; the ordinate scale applies to the lowest set of curves. We have not included the error bands of Fig. 14 or 16 in Figs. 18 and 19. In judging the quality of the fit, one must keep the error bands in mind. Each curve is labeled with the appropriate value of x and y.

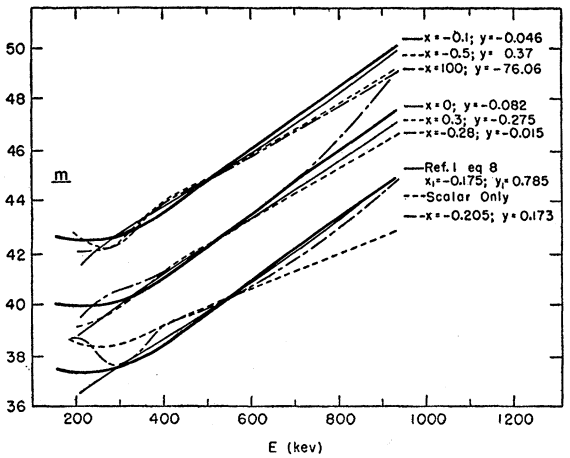

FIG. 18. Main inner group in Re^{186}. Comparison of experimental and theoretical shape factors. Solid curves are tracings of "best fit" curve of Fig. 14 (experimental shape correction factor). Lighter curves are theoretical shapes calculated with indicated values of nuclear matrix element ratio parameters x and y. Middle group of curves is shifted vertically by 3.6 ordinate units and top group by 7.2 ordinate units; scale applies to lower group.

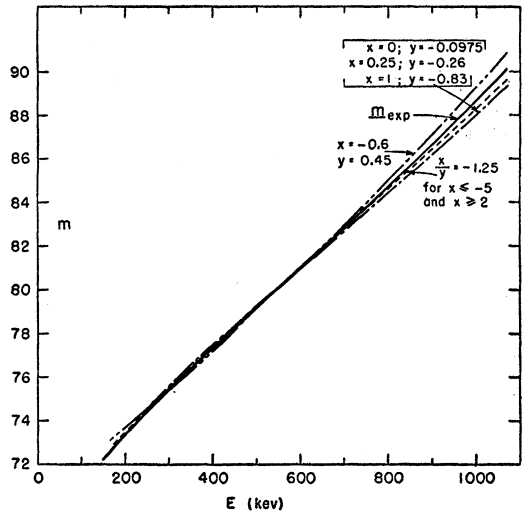

FIG. 19. Re^{186} ground-state transition. Comparison of experimental and theoretical shape factors. Solid curve is tracing of "best fit" curve of Fig. 16 experimental shape correction factor. Lighter curves are theoretical shapes calculated with indicated values of nuclear matrix element ratio parameters x and y.

In each of Figs. 17(a) and 17(b) the overlap area (cross hatched) is seen to extend (in fact, infinitely) to both positive and negative values of x, along straight lines. Theoretical shape factor curves calculated for points far out on these lines give satisfactory fits to the data, differing only slightly from the curves calculated for the indicated outermost points in Figs. 17(a) and 17(b). In Fig. 19 we show one curve calculated for (x,y) points on the line $x/y=-1.25$, which for $x>2$ or $x<-5$ lies well within the extrapolated overlap bands of Fig. 17(b). The implication of the good fits obtained for these high values of x and y for both transitions is that the matrix element $\int\beta\sigma\times\mathbf{r}$ need not contribute to these beta transitions.

One curve in Fig. 19 represents the almost indistinguishable fits of three distinct points in Fig. 17(b), $(0,-0.0975)$, $(0.25,-0.26)$, and $(1,-0.83)$.

In Fig. 18 one curve has been computed with the more approximate Eq. (8) of Mahmoud and Konopinski.[1] It is seen that although the point (x,y)[68] is outside the bands of Fig. 17(a) [and hence would give a poor fit using Eq. (5)], a fit is obtained. The curve marked "scalar only" clearly shows the need for including substantial contribution from tensor interaction. The curves for $x=0$ (no scalar) in Figs. 18 and 19 show that a fair fit can be obtained with tensor interaction only.

With the sole exception of the "scalar only" curve, the fits to the inner group must be regarded as more than satisfactory at energy >300 kev; the calculated curves lie well within the error bands of Fig. 14. In Sec. V we noted that the flattening of the experimental

[68] Note that x and y are given. They are related to the parameters x_1 and y_1 of reference 1 by the equations $x_1=x$, $y_1=[2/(1+S)](y+1+x)$.

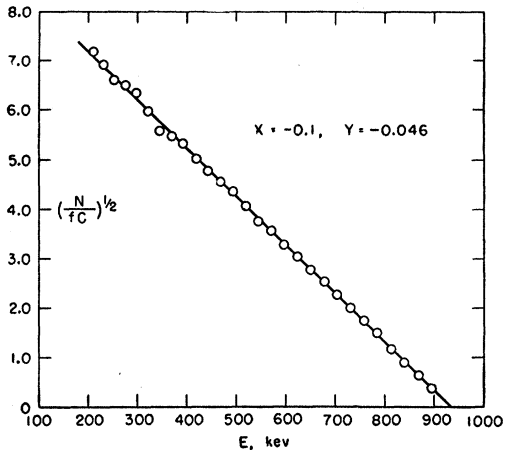

FIG. 20. Corrected Fermi-Kurie plot of main inner group of Re^{186}. The correction factor $C_{1ST}^{(1)}$ and the definition of the parameters x and y are given in Eqs. (2) to (5).

correction factor below 300 kev could not be due to the low-abundance 307-kev beta group, and thus the theoretical fitting actually is poorer below 300 kev than above. Two examples are shown, ($x=-0.205$, $y=0.173$) and ($x=-0.5$, $y=0.37$), of calculated $C_{1ST}^{(1)}$ which turn upwards above the experimental curve below 300 kev. All x,y pairs from the overlap area in the upper branch of the hyperbolas give such upward-deviating theoretical curves at low energies while the downward-turning theoretical curves arise from the overlap area on the lower branch of the hyperbolas. No overlap region exists which will give a theoretical curve lying between these extremes at low energy and better fitting the experimental data. Oscillations like those exhibited in the ($x=-0.5$, $y=0.37$) curve can occur since the U function employed is fifth degree in W owing to the inclusion of all the terms in the three-term expansion of L_0, M_0, and N_0. Inclusion of higher order terms in the series may reduce these oscillations. Some support of this may be found in the fact that recomputing this curve with tables of L_0, M_0, and N_0 extended to five-figure accuracy[69] eliminated the oscillations, while preserving the same general trend of the shape.

The relatively poorer fit obtained below 300 kev for the inner group compared to the ground state may reflect the omission of a possibly significant B_{ij} contribution for the former.

In Fig. 20 we show in an alternative representation of the fitting, the corrected Kurie plot for the inner group with $x=-0.1$ and $y=-0.046$. Any other x,y pair from the overlap regions of Fig. 17 would give Kurie plots which are just as straight.

[69] These five-figure values were obtained from raw data of the ORNL-1459 tables[62] kindly supplied to us by Dr. M. E. Rose. The existence of these more accurate data was discovered only after the computations of this section were complete.

VII. DISCUSSION

We have demonstrated that is is possible, within the stated theoretical approximations, to fit the experimental energy dependence of both abundant beta spectra in Re^{186} with a precision comparable to that obtained with allowed shapes with current beta spectroscopic techniques. We now show that for the inner group transition, the simultaneous theoretical fitting of the spectrum shape and of the beta-gamma angular correlation[25] serves to reject most of the range of the nuclear parameters for which a fitting of either separately is possible.

In a manner analogous to the solution of Eq. (6), the fitting of the angular correlation energy dependence proceeds graphically, resulting in conic section bands (as in Fig. 17) in x and y for each momentum p. These hyperbolas are shown in Fig. 4, reference 25. Only within the overlap areas of the bands of the latter figure [including (0.695, 0.035) and (−1.0, 0.58)] can fits be obtained for the angular correlation. Comparison[70] of these conics to those for the spectrum shape [Fig. 17(a)] shows no *common* overlap areas, but the overlap areas of both conic sets do approximate each other in the second quadrant. We have calculated the spectrum shape [Fig. 21(a)] and the correlation [Fig. 21(b)] for the (x,y) set, (−0.6, 0.44), selected at the point of closest approach of the overlap areas. The quality of the fit for the spectrum shape and for the angular correlation is not as good as for points selected within the overlap areas, particularly for the angular correlation, but is perhaps acceptable in each case.

In view of the recognized approximations in the theoretical development (omission of finite nuclear size effects, B_{ij} matrix element, other interactions, etc.), it is probably correct to regard this common "near" fitting as indicating that a theory including such refinements will probably fit both experiments more closely. However, the range in x,y for which there might be a common fitting would almost certainly differ from that found here. A relatively small shift in the x,y value is anticipated, by generalizing from the results of Yamada[2] on the small influence of finite nuclear size corrections in RaE and from Lee-Whiting's[4] calculations on the small effect associated with a factor-of-two change in nuclear radius value. This expectation is probably most optimistic with regard to the change in the angular correlation fitting associated with intro-

[70] The validity of the comparison is limited by the fact that slightly different electronic wave-function evaluations were used in computing the conic sets. Those for the angular correlation were the five-figure tables of Rose *et al.*[69] computed for mass number $A=189$; those for the spectrum shape were the Yamada[2] 3-term expansions using $A=186$. The mass number difference corresponds to a small (0.6%) difference in nuclear radius used. Some evidence that the influence of these differences is small is derived from the comparison of the theoretical shape factors for the point (−0.5, 0.37) described above.

ducing the βB_{ij} matrix element, inasmuch as it enters there linearly (in cross terms) as well as to second power, while only the squared term enters the spectrum shape factor. Since the βB_{ij} influence is small compared to $\int\beta\alpha$, the linear terms may be significant to the angular correlation where the squared terms are negligible in the shape factor. Indeed, some preliminary attempts[25] to include very small contributions of βB_{ij} interaction to the angular correlation fitting $[i\beta B_{ij}/\int\beta\sigma\times\mathbf{r}=\pm 0.1$, too small to affect the spectrum shape fitting significantly] resulted in marked changes in the overlap areas of the conics. A more refined attempt at simultaneous fitting must take the βB_{ij} interaction into account.

If, nevertheless, one assumes that the region in the x,y plane for which the inner group beta transition would be best fit is approximately located as found here near $(-0.6, 0.44)$, then some significance attaches to the following remarks.

For $y=0.44$, $\Lambda=(2\rho/\alpha Z)(\int\beta\alpha/\int\beta\sigma\times\mathbf{r})=0.90$. Rose and Osborn,[71] Ahrens and Feenberg,[72] and Pursey[60] predict Λ lies in the range 1 to 3.

The quantity G_S/G_T can be obtained from the value for x (-0.6) if the quantity $\epsilon=i(\int\beta\mathbf{r}/\int\beta\sigma\times\mathbf{r})$ is available. This latter can be estimated on the basis of the single-particle nuclear model if only one nuclear orbital is involved in the beta transition,[71,72] which may not be at all realistic for an odd-odd nucleus like Re^{186}, so far removed from shell edges. Assigning the proton and neutron orbitals as $h_{11/2}$ and $i_{13/2}$, respectively,[73] one obtains $\epsilon=-1$. Thus $G_S/G_T=+0.6$, in agreement with Lee-Whiting's[4] evaluation from the RaE analysis as regards sign and well inside his indicated range for the magnitude.

The fitting of the ground-state transition [Fig. 17(b)] gives equally good results with either sign of x, and hence furnishes no information on the sign of G_S/G_T. The theoretically predicted[60,71,72] range of Λ, 1–3, would be consistent with values of x in the range 0 to $+10$, using Eq. (3) and the relation $x/y=-1.25$ for which the ground state can be fit. Thus all high positive and all negative values of x would be rejected. For positive x, G_S/G_T is negative (for $\epsilon=-1$), in contrast to the result for the inner group. For $\Lambda<1$, however, G_S/G_T is positive, for $x/y=-1.25$.

Transitions to members of a rotational band have been discussed by Alaga *et al.*[74]; they predict, for transitions with the spin and parity sequence of the ground state and main inner group betas of Re^{186}, a ratio of 2.0 for the reduced transition probabilities. This probability varies inversely as f_1t for a first forbidden transition. The ratio of the f_0t values for these beta transitions in Re^{186} is 2.1 ± 0.2 assuming the beta multipolarity $L=1$. The error in the ratio is mainly that in the beta branching ratio. The ratio f_1/f_0 should be close to unity because of the small deviation from the allowed shape. Thus the transitions are consistent with the intensity rule. The similarity in spectrum shapes is perhaps correlatable by the collective model; the intensity relation indicates that the daughter states are pure rotational states, and thus $\Delta K=\Delta I=1$ for both transitions.

Quite in contrast is the f_0t value of the 307-kev beta transition to the 2+ level at 764 kev in Os^{186}, in relation to the ground state transition. Here the f_0t ratio is about 20, where the daughter states are not members of the same rotational band, even though the spins of this level and of the 137-kev level are the same.

It is noteworthy that preliminary work on the beta

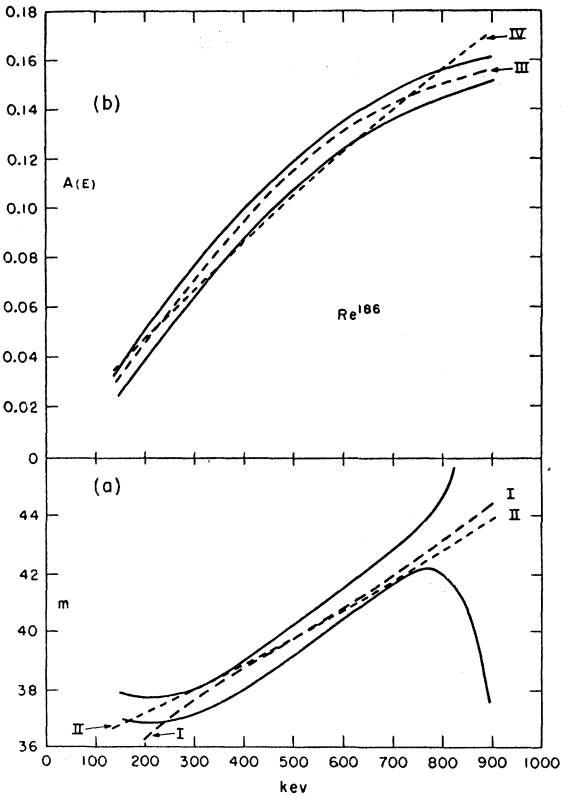

FIG. 21. (a) Spectrum shape correction factor for inner group of Re^{186} *vs* beta energy. Solid curves are experimental error bands of Fig. 14. Dashed curve (I) is theoretical shape for a point in the overlap region of Fig. 17(a) ($x=-0.1$, $y=0.046$). Dashed curve (II) is the theoretical shape for the point of closest approach of the shape factor and angular correlation conics, $(-0.6, 0.44)$, computed with the five-figure tables of Rose *et al.*[69] (b) β–γ angular correlation for Re^{186} *vs* beta energy. Solid curves are experimental error bands of Fig. 3, reference 25. Dashed curve (III) is theoretical correlation for a point in the overlap region of the "correlation conics", (0.695, 0.035). Dashed curve (IV) is the correlation for the point $(-0.6, 0.44)$.

[71] M. E. Rose and R. K. Osborn, Phys. Rev. **93**, 1326 (1954).
[72] T. Ahrens and E. Feenberg, Phys. Rev. **86**, 64 (1952).
[73] P. F. A. Klinkenberg, Revs. Modern Phys. **24**, 63 (1952).
[74] Alaga, Alder, Bohr, and Mottelson, Kgl. Danske Videnskab. Selskab, Mat.-fys. Medd. **29**, No. 9 (1955).

spectrum of Re^{188} gives indication[22] of similar concave downward deviations from the allowed shape for the transitions to ground and first excited states of Os^{188}. We are pursuing investigation of the isotope, and of Tm^{170}, searching for smaller deviations than have thus far been sought in the latter. We feel also that a more careful investigation of the shape of the main transition in Au^{198} is merited.

ACKNOWLEDGMENT

We wish to thank Gordon Goodman for his assistance with some of the computations.

PHYSICAL REVIEW VOLUME 103, NUMBER 4 AUGUST 15, 1956

Beta-Gamma Directional Correlation in Re^{186}†

T. B. NOVEY, M. S. FREEDMAN, F. T. PORTER, AND F. WAGNER, JR.
Argonne National Laboratory, Lemont, Illinois

(Received January 9, 1956)

The directional correlation between the nonunique first forbidden 934-kev beta group and the 137-kev $E2$ gamma transition in the decay of Re^{186} has been measured as a function of beta energy above 150-kev. Analysis of the experimental data included a correction for the finite energy resolution of the anthracene crystal scintillation spectrometer, which takes into account the effect of the backscattering of electrons from the crystal. The differential anisotropy increases with increasing beta energy to 0.158 ± 0.006. The directional correlation $W(\theta)=1+(0.105\pm0.003)\cos^2\theta$ for beta energies of 257–934 kev, with no evidence for a $\cos^4\theta$ term, in agreement with theoretical expectation for a first forbidden beta transition.

Limited ranges for the ratios of the nuclear matrix elements governing the beta decay were obtained by comparison with theory, assuming the following: the spin and parity sequence $(1-, 2+, 0+)$; the beta interaction mixture scalar plus tensor; point nuclear charge. Higher order terms in $2\rho/\alpha Z$ were included.

I. INTRODUCTION[1]

CONCURRENT with the investigation[2] of the shape of the beta distribution of 89-hr Re^{186}, a study was made of the directional correlation of the 934-kev beta branch with the 137-kev gamma.[3] The primary purpose of this experiment was to secure an independent determination of the nuclear matrix element ratios governing this beta decay, for comparison to those derived from beta spectroscopy. An added motive was to obtain a measurement of the correction to be applied to the magnetic spectrometer coincidence data to derive the "integrated over 4π solid angle" spectral shape. We measured both the differential (with beta energy) and integral correlations.

In the only previously reported[4] measurements of this beta-gamma directional correlation, an upper limit of 0.07 was set on the anisotropy.

The decay scheme[5] of Re^{186} is given in Fig. 1, reference 2. The 137.2-kev gamma ray is known to be $E2$ in character from the L-subshell relative conversion ratios,[6] from the K-conversion coefficient,[2,5] and from the 627-kev gamma–137-kev gamma angular correlation.[4] The lifetime of the lower $2(+)$ state in Os^{186} is 0.8×10^{-9} seconds.[7] From the first forbidden character of the 934-kev beta transition and the pure $E2$ character of the 137-kev gamma ray, a correlation function $W(\theta)$ of the form

$$W(\theta)=1+A(E)\cos^2\theta \qquad (1)$$

is anticipated, neglecting contributions from third and higher order forbidden terms.

II. EXPERIMENTAL

A. Apparatus

The sources were prepared from the identical supply of neutron activated and aged $KReO_4$ as used for the spectrometer sources,[2] and were similarly volatilized in vacuum onto 200 $\mu g/cm^2$ Al foils. Average source thickness over the $\frac{1}{4}$-inch diameter sources was 12 $\mu g/cm^2$. The foils were mounted on a 2-in. diameter thin aluminum ring to minimize source mount scattering.

The source holder was centered in a chamber[8] 7 in. in diameter and 7 in. high with $\frac{1}{8}$ in. thick Bakelite walls, which was evacuated to about 1 mm Hg. The plane of the source was oriented at 45° to the beta direction.

The $\frac{1}{4}$-in. thick by $1\frac{1}{4}$-in. diameter anthracene beta

† Based on work performed under the auspices of the U. S. Atomic Energy Commission.

[1] For an extended discussion of some of the details of this paper, see Novey, Freedman, Porter, and Wagner, Argonne National Laboratory Report ANL–5523, February, 1956 (unpublished).

[2] Porter, Freedman, Novey, and Wagner, Phys. Rev. **103**, 921 (1956), preceding paper.

[3] Preliminary reports of these experiments have been given; Porter, Freedman, Novey, and Wagner, Phys. Rev. **98**, 214 (1955); and Phys. Rev. **99**, 671(A) (1955).

[4] J. P. Hurley and P. S. Jastram, Phys. Rev. **95**, 627 (1954).

[5] F. R. Metzger and R. D. Hill, Phys. Rev. **82**, 646 (1951); R. M. Steffen, Phys. Rev. **82**, 827 (1951).

[6] J. B. Swan and R. D. Hill, Phys. Rev. **91**, 424 (1953).

[7] F. K. McGowan, Phys. Rev. **81**, 1066 (1951).

[8] T. B. Novey, Phys. Rev. **89**, 672 (1953).